

THE BAND STRUCTURE OF CdO

by

ALAN LEAVER, B.Sc.

A Thesis

Submitted to the School of Graduate Studies  
in Partial Fulfilment of the Requirements  
for the Degree  
Master of Science

Brock University

March 1978

© Alan Leaver 1978

#### ACKNOWLEDGEMENT

I wish to express my thanks to my supervisor,  
Dr. E. R. Cowley for his guidance and assistance  
during this project.

MASTER OF SCIENCE

(Physics)

BROCK UNIVERSITY

St. Catharines, Ontario.

TITLE: The Band Structure of CdO

AUTHOR: Alan Leaver, B.Sc. (Brock University)

SUPERVISOR: Dr. E. R. Cowley

NUMBER OF PAGES: 70

SCOPE AND CONTENTS:

The Augmented Plane Wave Method has been used to calculate the one-electron energy band structure of CdO. Energy eigenvalues were calculated along three symmetry lines and for some other general wave-vectors of interest.

## TABLE OF CONTENTS

<u>Chapter</u>	<u>Title</u>	<u>Page</u>
I	INTRODUCTION	1
	Energybands	1
	Energy Gaps	3
	General Background	6
II	GENERAL THEORY	11
III	THE NEUTRAL CALCULATION	20
	The Potential	20
	The Logarithmic Derivatives	36
	The Determinant	37
IV	THE IONIC CALCULATION	44
V	DISCUSSION AND CONCLUSION	68
	BIBLIOGRAPHY	70

## LIST OF ILLUSTRATIONS

<u>Figure</u>	<u>Title</u>	<u>Page</u>
1.1	Direct and Indirect Transitions.	5
1.2	Brillouin Zone for the face centred cubic lattice.	7
2.1	The $n^{\text{th}}$ unit cell atomic site and APW potential for a direction in a two-dimensional lattice in which the Muffin-Tin spheres do not touch.	12
3.1	Plot of crystal potential versus distance from nuclei.	35
3.2	Logarithmic derivatives for neutral Cadmium.	38
3.3	Logarithmic derivatives for neutral Oxygen.	40
4.1	Energy bands in $\Sigma$ direction.	60
4.2	Energy bands in $\Lambda$ direction.	61
4.3	Energy bands in $\Delta$ direction.	62
4.4	Schematic plot of density of states for two maxima in valence band and for one maximum and a saddle point.	63

# LIST OF TABLES

<u>Number</u>	<u>Title</u>	<u>Page</u>
3.1	Comparison of Herman Skillman and Clementi charge densities on H.S. grid.	25
3.2	Comparison of Herman Skillman and Clementi charge densities on Louck's grid.	26
3.3	Number of atoms and distance from central atom of surrounding shells.	29
3.4	Comparison of results obtained through the variation of the $\alpha$ value in the exchange correction.	30
3.5	Cadmium potential for neutral crystal.	31
3.6	Oxygen potential for neutral crystal.	33
3.7	Convergence of energy eigenvalues at $\Gamma$ for neutral calculation.	43
4.1	Cadmium potential for ionic crystal.	51
4.2	Oxygen potential for ionic crystal.	53
4.3	Logarithmic derivatives for ionic cadmium.	55
4.4	Logarithmic derivatives for ionic oxygen.	57
4.5	Convergence of energy eigenvalues at $\Gamma$ for ionic crystal.	59

<u>Number</u>	<u>Title</u>	<u>Page</u>
4.6	Energy eigenvalues in directions perpendicular to maxima in $\Sigma$ and $\Delta$ symmetry axes.	64
4.7	Band shapes and effective masses of conduction band around $\Gamma$ .	65
4.8	Band shapes and effective masses of valence band around $\Gamma$ .	66
4.9	Effective masses at $L$ .	67

# CHAPTER I

## INTRODUCTION

### Energybands

An understanding of energy band structure is a valuable tool when one is considering the optical and electrical properties of crystalline materials.

A crystal structure may be considered as consisting of two components. There is the crystal lattice which is a regular periodic arrangement of points in space and associated with this are the primitive translation vectors  $\vec{a}$ ,  $\vec{b}$ , and  $\vec{c}$ . These are required to define a vector

$$\vec{T} = n_1 \vec{a} + n_2 \vec{b} + n_3 \vec{c} \quad (1.1)$$

where  $\vec{T}$  can move any lattice point into every other lattice point by a suitable choice of integer values for  $n_1$ ,  $n_2$ , and  $n_3$ . To complete the structure a basis of atoms must be added in an identical fashion to each of these lattice points. These basis atoms may be regarded as ionic cores which consist of the nucleus and the inner core electrons which remain virtually unchanged and the outer atomic orbitals. When these outer atomic orbitals are brought within close proximity of each other with the creation of the crystal the resulting overlap creates bands consisting of extremely closely spaced energies.

If  $N$  is the number of unit cells in the crystal being considered then  $2N$  is the maximum number of electrons any of the energy bands can hold. The number of electrons available to fill the bands depends on the type of atoms in the crystal as does the spacing of the bands relative to each other. The region between bands corresponds to the energies which are "forbidden"

to the electrons and these are called energy gaps. In metals some bands are only partially full of electrons and these will readily conduct a current. If all the bands are either full or empty and there is a large gap between the last full band (valence band) and the first empty band (conduction band) the crystal will not conduct current and is called an insulator. If the gap between the valence and conduction bands is relatively narrow then the crystal is a semiconductor. In an intrinsic semiconductor, thermal excitation will cause electrons in the valence band to cross the gap into the conduction band. The departure of the electron from the valence band creates a "hole" which can act as a positive current carrier. Consequently there is a one to one pairing between the number of free electrons and the number of holes. Extrinsic semiconductivity may arise from donor impurities or defects yielding more electrons than the valence band can hold. The surplus electrons are then available to occupy the conduction band. Alternately, acceptor impurities or defects can create holes in what would otherwise have been a full valence band. Crystals containing these two types of impurities or defects are called n-type or p-type semiconductors respectively.

Optical properties are also related to the energy band structure. If a band is not full, then low frequency light will be absorbed, exciting the electrons between different levels in the same band. Insulators require high energy light to excite electrons across the large band gap and consequently are usually transparent to visible light. Semiconductors will absorb light

at lower energies than insulators and the lowest energy to be absorbed depends on the width of the energy gap between the conduction and valence bands.

### Energy Gaps

Transitions across energy gaps can occur by way of one of three mechanisms related to optical absorption. The first of these is called a direct transition and the other two are indirect transitions. It is necessary to digress slightly here in order to provide a more complete explanation of these terms.

One electron energy band calculations result from the solution of the single electron approximation of the Schrödinger equation which describes the motion of an electron in a periodic lattice. This equation is written as

$$H \psi_{\vec{k}}(\vec{r}) = [-\nabla^2 + V(\vec{r})] \psi_{\vec{k}}(\vec{r}) = E_{\vec{k}}(\vec{r}) \psi_{\vec{k}}(\vec{r}) \quad (1.2)$$

here atomic units have been used so the energy is in rydbergs, and distances are in Bohr radii (note 1 ryd = 13.605826eV, 1Bohr radius = 0.529167Å°). This will be the case for all calculations in this work. The potential  $V(\vec{r})$  represents the summed coulombic affects of the ionic cores plus an averaged value for the electron's interaction with the rest of the conduction electrons. It also exhibits the periodicity of the crystal, that is, it is required to remain invariant under a lattice translation  $\vec{T}$ ,

$$\text{ie } V(\vec{r} + \vec{T}) = V(\vec{r}) \quad (1.3)$$

where  $\vec{T}$  is given by (1.1). As the potential is periodic,

Bloch's Theorem may be applied, hence the eigenfunctions of the wave equation are of the form

$$\psi_{\vec{k}}(\vec{r}) = e^{i\vec{k}\cdot\vec{r}} U_{\vec{k}}(\vec{r}) \quad (1.4)$$

where  $U_{\vec{k}}(\vec{r})$  is to have the periodicity of the lattice and  $\vec{k}$  is a wavevector describing the state of the electron.

Consequently,  $E_{\vec{k}}$  can be calculated for different wavevectors  $\vec{k}$  and a plot of  $E$  vs  $\vec{k}$  will yield the required energy bands and gaps.

The reduced zone scheme will be used, hence only the values of  $\vec{k}$  in the first Brillouin Zone need be considered. This results from the fact that any wavevector  $\vec{k}$  outside the first BZ can always be reduced to a vector  $\vec{k}$  inside the zone by subtracting a suitable reciprocal lattice vector  $\vec{G}$ .

$$\vec{k} = \vec{k}' - \vec{G} \quad (1.5)$$

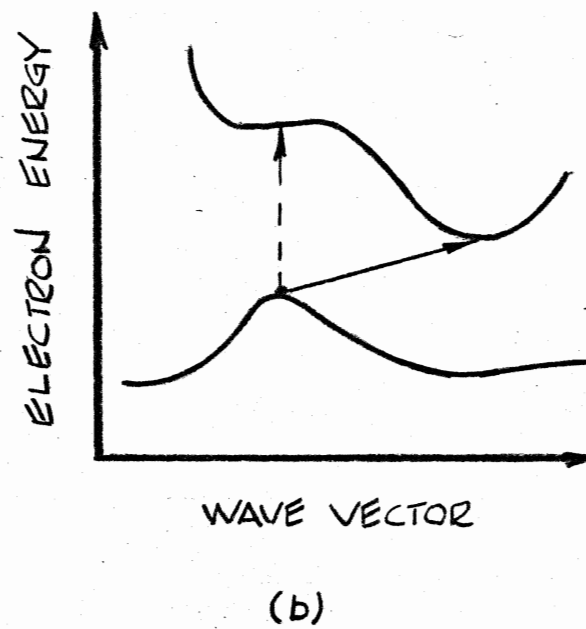
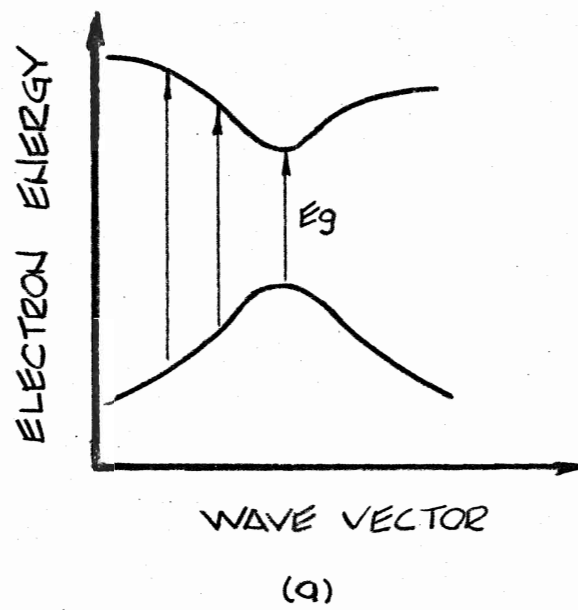
Figure 1 gives an illustration of direct and indirect transitions. Diagram "a" represents a transition in energy with no appreciable change in wavevector. Transitions of this type are called direct transitions and the lowest energy of light absorbed is equal to the band gap. Diagram "b" illustrates an indirect transition which involves a change in wavevector and energy. This change must be accompanied by the creation or annihilation of a phonon. In the case of phonon creation the photon energy is greater than the band gap by an amount equal to that of the phonon. If a phonon is annihilated then the photon energy is less than the band gap by an amount equal to the phonon energy.

Figure 1.1

a) Direct Transition

b) Indirect Transition (solid arrow)

Figure 1.1

Fig (1.1)

## General Background

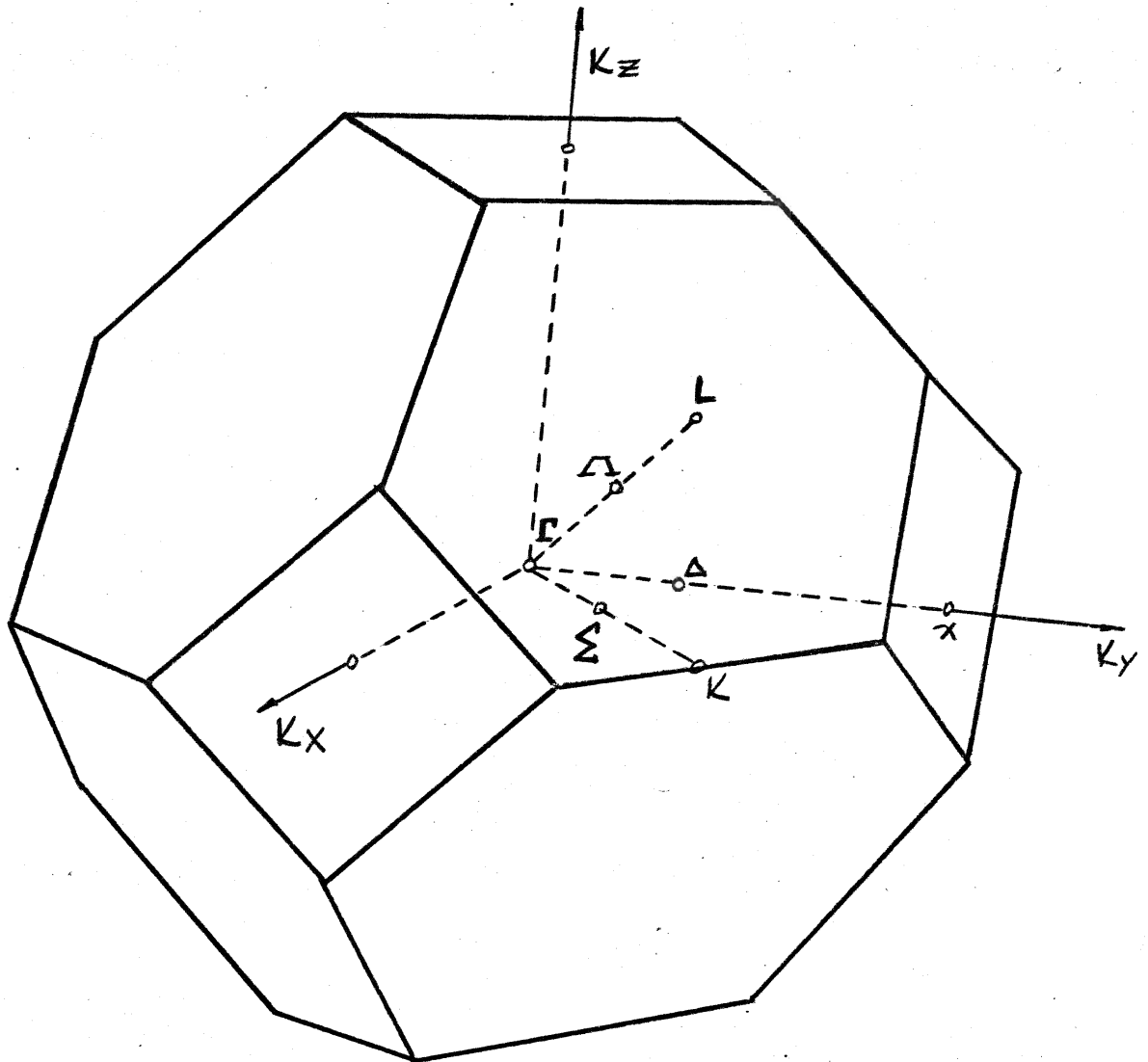
Cadmium oxide is a II-VI Compound which crystalizes only into a rocksalt lattice. It is an n-type semiconductor with nearly metallic conductivity resulting from either cadmium interstitials or oxygen vacancies (Koffyberg, 1975). It has been the object of considerable investigation in the past ten years.

Experimental work on single crystals and thin films has yielded varying results to confirm some of the theoretical work.

The work of the experimentalists in determining the indirect gap widths is greatly hampered by the presence of free electron concentrations. Altwein (1968) maintains that the indirect gaps, being around 1eV in magnitude will be undetectable in single crystals because the absorption by the free carriers will be too high. He reduced this free electron problem by working with sputtered thin films instead of single crystals. By changing preparation conditions the electron concentration could be reduced to  $10^{14}\text{cm}^{-3}$  from about  $10^{21}\text{cm}^{-3}$ . Using a thin film with concentration  $10^{16}\text{cm}^{-3}$  at 300°K, and extrapolating the linear portion of the absorption curve from between 1.9eV to 1.4eV, Altwein deduced an indirect gap of 1.2eV. He was unable to detect any other indirect gaps.

A second experimental attempt at finding the indirect gaps was made by Köhler (1972). Working with thin films at 300°K he determined that there was an indirect gap at 1.35eV and another at 0.55eV. Allowing for band gap variation with temperature the gaps were then calculated to be 1.5eV and 0.7eV at T=0. He also suggested that the existence of an impurity

FIGURE 1.2



BRILLOUIN ZONE FOR THE FACECENTRED  
CUBIC LATTICE

conduction band overlapping the conduction band may explain some of the discrepancies between the different experimental works.

Kocka (1971) looked for indirect transitions in single crystal CdO at 85°, 173°, and 296°K. He measured the absorption coefficient for an energy range of 0.5eV to 2.2eV and the results indicated an indirect gap at  $1.09 \pm .04$  eV. Again it was felt that the calculated gap about 0.8eV was not detectable because it was being masked by free electron absorption.

Koffyberg (1975) obtained the thermoreflectance spectra for single crystals. His results gave the direct gap of  $2.28 \pm .05$  eV and two indirect gaps of 0.84eV and 1.09eV. Furthermore, a comparison of single crystals and thin films appeared to indicate that the discrepancies in results were not caused by impurity bands as suggested previously by Kocka (earlier in this section) but were more likely the result of structural peculiarities. In addition to this, he questioned the validity of the parabolic shape of the  $\Gamma_1$  and  $\Gamma_{15}$  bands at the direct gap. These bands had been calculated by three theoretical works but only in high symmetry directions. Nothing was known about their behaviour in other directions.

The first theoretical calculation was performed by Maschke and Rossler (1968) using the Augmented Plane Wave Method (APW) incorporating the results of a selfconsistent potential calculation by Herman and Skillman (1963). The work was only performed along high symmetry axes in the Brillouin Zone. Energies were calculated in the  $\Delta$  direction from  $\Gamma$  to L ;

in the  $\Delta$  direction from  $\Gamma$  to  $X$  ; and in the  $\Sigma$  direction from  $\Gamma$  to  $K$  and on to  $X$  . These points and directions are shown in fig. (1.2). A parameter, the intersphere potential (discussed in chapter 2), was varied to fit the known direct optical gap of 2.35eV. The results showed two indirect gaps. One from the maximum at  $L$  in the valence band to the minimum which occurs at  $\Gamma$  in the conduction band. The other was from the maximum in the  $\Sigma$  direction to the conduction band minimum at  $\Gamma$  .

The APW method was also used by Tewari (1973) to calculate the energy bands along the same symmetry axes as Maschke and Rössler. Instead of fitting any parameters to experimental data, she calculated the bands twice. First, she performed a neutral calculation assuming no electron exchange between the atoms, and secondly she performed an ionic calculation assuming an ionicity of +1 for cadmium and -1 for oxygen. The neutral calculation predicted metallic behaviour while the ionic calculation gave results very similar to those of Maschke and Rössler. Since we could not duplicate her neutral calculation and since a request to her for further information in 1977 has met with no reply to date we put very little trust in the accuracy of her work.

A Linear Combination of Atomic Orbitals (LCAO) calculation was done by Breeze and Perkins (1973) by parameterizing initially to atomic values and then fitting the direct gap. The overall shape of the resulting bands is similar to Maschke's and Tewari's ionic calculation but the indirect gaps are much

closer together. The  $\Gamma-L$  gap is 1.18eV and the  $\Gamma-\Sigma$  gap is 1.12eV.

These three theoretical calculations are weak in several areas. Firstly the energy bands are only calculated in the  $\Lambda$ ,  $\Delta$  and  $\Sigma$  directions. Consequently there is insufficient information to determine whether the maxima in the valence bands are local maxima or just saddle points. Since the optical properties for two local maxima would be different from a maxima and a saddle point, it is necessary to know which structure exists. This information would be helpful to the experimentalists in interpreting their results. Secondly, none of the papers investigated in detail the shape of the conduction and valence bands around  $\Gamma$  or calculated the effective masses characterizing the maxima in the valence band and the minimum in the conduction band. This is important since these parameters must be known before the optical properties can be predicted. Thirdly, these previous works have treated the calculations in a more unphysical fashion than is actually necessary. Since cadmium oxide is known to be highly ionic, and since the shape and separation of the energy bands will depend on the degree of this ionicity, the importance of this dependence should be investigated and could perhaps be used to create a more realistic model for the calculation. The aim of this work is to perform a detailed APW calculation of the energy bands around the maxima and minimum of interest. This information will then be used to calculate representative effective masses. The effect of ionicity will also be investigated and incorporated into the calculation.

## CHAPTER II

### GENERAL THEORY

The Augmented Plane Wave method of band calculation was originally formulated by Slater (1937). However, the method was intractable and it was not until the 1960's when high speed computers became generally available that the method became computationally feasible. The method was modified twice before the 1960's in an effort to reduce the prohibitive calculation time, but by the mid 1960's it was found through the experience of different workers that the original formation was after all, most appropriate.

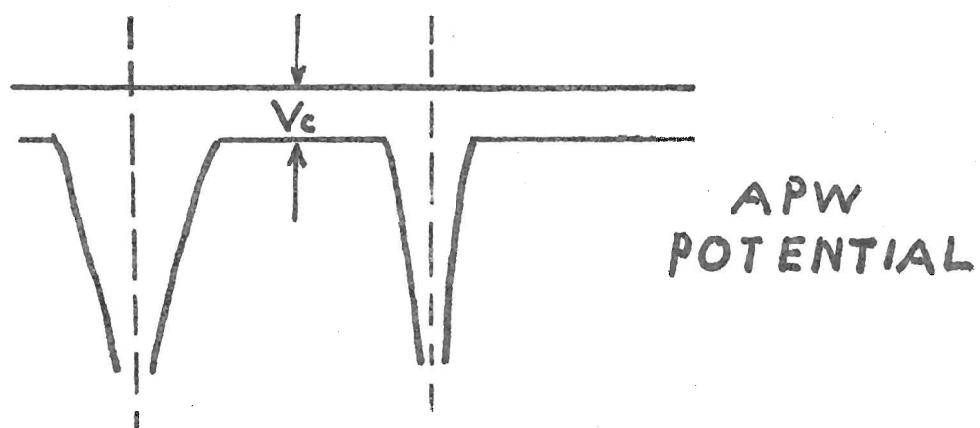
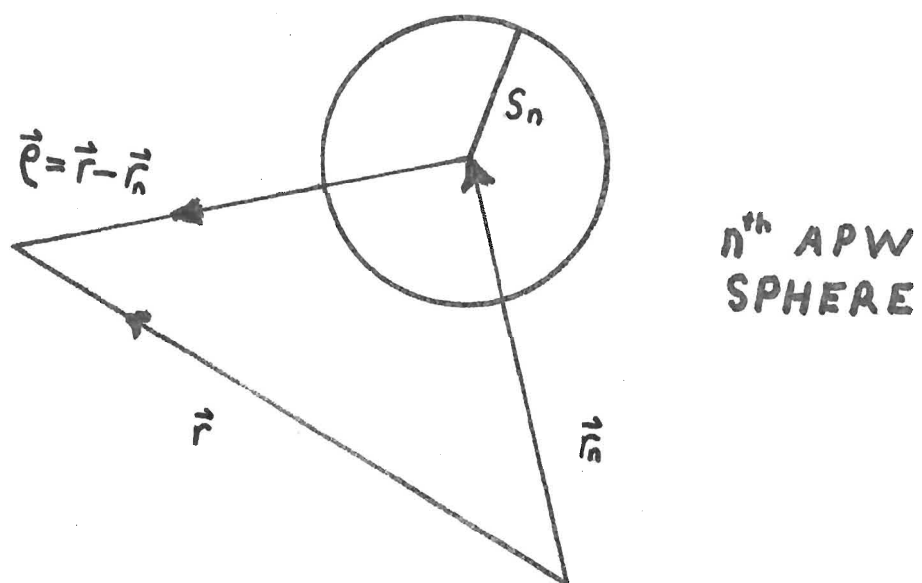
To obtain the solutions of equation (1.2) using the one electron approximation Slater (1937) made the assumption that the actual crystal potential required in equation (1.2) could be approximated in the following way. The potential around the atomic sites is to be spherically symmetric out to a radius  $S_n$ , (see Fig. 2.1). The subscript  $n$  is necessary if there are more than one type of atom in the unit cell since each must have it's own corresponding sphere radius. The only restrictions on the size of the spheres of symmetric potential are that they do not overlap and that the value of the potential should be continuous across the sphere boundaries. The value of the potential in the region between the spheres is usually considered as constant although small variations can be handled as perturbations (De Cicco (1965)). Because the spherically symmetric potentials around the atomic sites are considered to be better approximations than the constant intersphere potential, it is desirable to choose the sphere radii as large as possible.

Figure 2.1

The  $n^{\text{th}}$  unit cell atomic site or APW sphere  
showing the convention of symbols used in the  
calculations

APW or Muffin-Tin potential for a direction in  
a two-dimensional lattice in which the spheres do  
not touch

Figure 2.1



The origin of the potential scale is chosen to set the intersphere potential  $V_c$  (Fig. 2.1) at zero. The potential within the spheres is then shifted accordingly. Inspection of the potential shown in figure 2.1 may give some indication of why Slater chose to call it a "muffin-tin" potential.

Having postulated the "muffin tin" form of the potential for the crystal, Slater then suggested that the crystal wave function  $\Psi$  be the sum of linearly independent functions  $\chi^i$ .

$$\Psi = \sum_{i=1}^M c_i \chi^i \quad (2.1)$$

where  $\chi^i = \chi(\vec{k} + \vec{g}_i)$

The  $\vec{g}_i$  are the reciprocal lattice vectors of the structure under consideration and the  $c_i$  are coefficients to be determined variationally. In the intersphere regions where the potential was set at zero the  $\chi^i$  could be represented by a plane wave, but it was known that it is very difficult to approximate the wave function near the atomic nuclei by even a large sum of plane waves. Slater then suggested letting the  $\chi^i$  have two forms: Inside the spheres a linear combination of atomic orbitals and outside a plane wave. It should be pointed out though that the consequence of this appears in the evaluation of the kinetic energy which will be discussed later in this section. Each  $\chi^i$  is a plane wave augmented by a more suitable type of solution within the spheres and hence the name Augmented Plane Wave.

Now more specifically it is known that inside the regions of the spherically symmetric potential the Schroedinger equation

is satisfied by a function of the form

$$\psi_{lm}(\theta, \phi, \rho) = A_{lm} Y_{lm}(\theta, \phi) R_{ln}(\rho, E) \quad (2.2)$$

where the  $A_{lm}$  are arbitrary constants at this point and

$Y_{lm}(\theta, \phi)$  are the spherical harmonics for the azimuthal and magnetic numbers  $l$  and  $m$  respectively. The functions  $R_{ln}(\rho, E)$  are solutions of the radial Schroedinger equation

$$-\frac{1}{\rho^2} \frac{d}{d\rho} \left( \rho^2 \frac{dR_{ln}}{d\rho} \right) + \left[ \frac{l(l+1)}{\rho^2} + V_n(\rho) \right] R_{ln} = E R_{ln} \quad (2.3)$$

The coordinate  $\rho$  has its origin at the centre of the  $n^{\text{th}}$  sphere as shown in figure 2.1 and  $V_n(\rho)$  is the potential inside this sphere. The only restriction placed on the form of the solutions

$R_{ln}(\rho, E)$  is that they be regular at the origin. It is not required to satisfy any boundary conditions at the sphere surface and consequently the energy  $E$  remains arbitrary.

In the region of zero potential between the spheres each  $\chi^i$  is to take the form of a plane wave.

$$\begin{aligned} \text{ie. } \chi^i &= e^{i\vec{k}_i \cdot \vec{r}} \\ &= e^{i\vec{k}_i \cdot (\vec{r}_n + \vec{\rho})} \\ &= e^{i\vec{k}_i \cdot \vec{r}_n} e^{i\vec{k}_i \cdot \vec{\rho}} \end{aligned}$$

$$\text{where } \vec{k}_i = \vec{k} + \vec{q}_i$$

and  $\vec{r}$  and  $\vec{r}_n$  are shown in Fig. (2.1). The plane wave  $e^{i\vec{k} \cdot \vec{\rho}}$  may be expanded in spherical harmonics (Powell and Crassman, 1961) in the following manner:

$$e^{i\vec{k} \cdot \vec{\rho}} = 4\pi \sum_{l=0}^{\infty} \sum_{m=-l}^{+l} i^l Y_{lm}^*(\hat{k}) Y_{lm}(\hat{\rho}) j_l(k\rho)$$

where  $\hat{k}$  and  $\hat{e}$  are the angular parts of the vectors  $\vec{k}$  and  $\vec{e}$ . The  $j_l(kr)$  are the spherical Bessel Functions. The general APW function has the form

$$\chi^i = \sum_{l=0}^{\infty} \sum_{m=-l}^{+l} A_{lm} Y_{lm}(\theta, \phi) R_{lm}(r, E) \quad (2.4)$$

inside the spheres and

$$= e^{i\vec{k} \cdot \vec{r}_n} \left[ 4\pi \sum_{l=0}^{\infty} \sum_{m=-l}^{+l} Y_{lm}^*(\hat{k}_i) Y_{lm}(\hat{e}) j_l(k_i r) \right] \quad (2.5)$$

outside the sphere. To maintain continuity of the wave function  $\chi^i$  at the sphere boundary  $S_n$ , comparison of equations (2.4) and (2.5) yields

$$A_{lm} = 4\pi e^{i\vec{k}_i \cdot \vec{r}_n} i^l Y_{lm}^*(\hat{k}_i) \frac{j_l(k_i S_n)}{R_{nl}(S_n, E)}$$

but the discontinuity in the slope of  $\chi^i$  still remains and will be discussed later in connection with the evaluation of matrix elements. The crystal wave function is assumed to be a linear combination of these APW's

ie.  $\Psi = \sum_{i=1}^N c_i \chi^i$

Straightforward application of the variational method leads to

$$\text{Det} (H-E)_{ij} = 0$$

where  $(H-E)_{ij} = \int \chi^{i*} (H-E) \chi^j d\tau$

The problem of setting up the general matrix element is complicated by the fact that the individual APW's have a discontinuity in slope at the sphere boundaries and integration across this discontinuity will yield an extra contribution to the kinetic energy. Slater (1937) was able to allow for this discontinuity of slope by using Schroedinger's original

representation of the kinetic energy instead of the more common

$-\nabla^2$  form which only applies to continuous differentiable functions. Hence, instead of evaluating  $\int \chi^{i*} (-\nabla^2) \chi^j d\tau$  he used the more basic form  $\int \text{grad } \chi^{i*} \cdot \text{grad } \chi^j d\tau$

The general matrix element results from evaluating

$$\int \chi^{i*} (H-E) \chi^j d\tau$$

over the volume of the cell and dividing the result by the cell volume  $\Omega$  to get the average value per unit volume.

To evaluate this integral consider the cell as containing two regions and determine the contribution from each. In region I which is to include the spheres and their surfaces the Hamiltonian consists of the dot product of the gradients of the functions plus the spherically symmetric potential. The X's have the form of equation (2.5). Region II is outside the spheres and excludes the spherical surfaces. The potential is zero in this region and the X's are individual plane waves. To obtain the contribution from region II, first integrate over the entire cell and then over the spheres contained within the cell, and finally subtract the latter from the former.

#### Contribution To Matrix Element From Region II

Because the potential is zero in this region the matrix element  $(H-E)_{ij}$  is given by  $\frac{1}{\Omega} \int_{\text{cell}} (\text{grad } \chi^{i*} \cdot \text{grad } \chi^j - E \chi^{i*} \chi^j) d\tau$   
Step 1 integration over the unit cell yields:

$$\begin{aligned} & \frac{1}{\Omega} (\vec{k}_i \cdot \vec{k}_j - E) \int_{\text{cell}} \chi^{i*} \chi^j d\tau \\ &= (\vec{k}_i \cdot \vec{k}_j - E) \delta_{ij} \\ &= (k_i^2 - E) \end{aligned}$$

Step 2 integration over the  $n^{\text{th}}$  sphere:

$$\frac{1}{\pi} (\vec{k}_i \cdot \vec{k}_j - E) e^{i(\vec{k}_j - \vec{k}_i) \cdot \vec{r}_n} \int_0^{S_n} e^{i(\vec{k}_j - \vec{k}_i) \cdot \vec{r}} d\tau$$

$$= \frac{1}{\pi} (\vec{k}_i \cdot \vec{k}_j - E) e^{i(\vec{k}_j - \vec{k}_i) \cdot \vec{r}_n} \left( 4\pi S_n^2 \frac{\mathcal{J}_1(|\vec{k}_j - \vec{k}_i| S_n)}{|\vec{k}_j - \vec{k}_i|} \right)$$

ie: the contribution from the region between the spheres is

$$(k_i^2 - E) \delta_{ij} \leq \frac{4\pi S_n^2}{\pi} (\vec{k}_i \cdot \vec{k}_j - E) e^{i(\vec{k}_j - \vec{k}_i) \cdot \vec{r}_n} \frac{\mathcal{J}_1(|\vec{k}_j - \vec{k}_i| S_n)}{|\vec{k}_j - \vec{k}_i|}$$

### Contribution To Matrix Element From Region I

In region I the X's have the form of equation (2.4) and the contribution to the matrix element for the  $n^{\text{th}}$  sphere is

$$\frac{1}{\pi} \int_0^{S_n} (\text{grad } \chi^{i*} \cdot \text{grad } \chi^j + (V_n(\rho) - E) \chi^{i*} \chi^j) d\tau$$

Now applying the result

$$\int_0^{S_n} \vec{\nabla} \chi^{i*} \cdot \vec{\nabla} \chi^j d\tau = \int_0^{S_n} \chi^{i*} (-\nabla^2) \chi^j d\tau + \int_{\text{surface}} \chi^{i*} \left( \frac{\partial \chi^j}{\partial n} \right) dS$$

the above becomes

$$\frac{1}{\pi} \left\{ \int_0^{S_n} \chi^{i*} (-\nabla^2 + V_n(\rho) - E) \chi^j d\tau + \int_{\text{surface}} \chi^{i*} \left( \frac{\partial \chi^j}{\partial n} \right) dS \right\}$$

where  $dS = S_n^2 \sin \theta d\theta d\phi$  and  $n$  is in the direction of the outward normal from the  $n^{\text{th}}$  sphere.

In determining the functions  $\chi^i$  it is necessary to solve the radial Schroedinger Equation and the solutions  $R_{ln}(\rho, E)$  depended upon the arbitrary choice of energy E. Denoting the choice of energy as  $E'$  the resulting APW satisfied the equation

$$(-\nabla^2 + V_n(\rho)) \chi^i = E' \chi^i$$

or

$$(-\nabla^2 + V_n(\rho) - E') \chi^i = 0$$

It is clear then that if  $E'$  is chosen equal to the characteristic

energy  $E$  in equation (2.3) then the volume integral becomes zero. This means the APW's will depend on the energy  $E$  contained within the problem

$$\text{Det} (H - E)_{ij} = 0$$

which is exactly the problem to be solved; however, this complication is outweighed by the simplification obtained by eliminating the volume integral.

Now we evaluate the remaining surface integral by differentiating (2.4) with respect to  $\epsilon$  and integrate over the angles to obtain

$$\int_{\text{surface}} \chi^{i*} \left( \frac{\partial \chi^j}{\partial n} \right) dS = e^{i(\vec{k}_j - \vec{k}_i) \cdot \vec{r}_n} \frac{4\pi S_n^2}{\Omega} \sum_{\ell=0}^{\infty} (2\ell+1) P_{\ell}(\vec{k}_i \cdot \vec{k}_j) g_{\ell}(k_i S_n) g_{\ell}(k_j S_n) \frac{R'_{n\ell}(S_n, E)}{R_{n\ell}(S_n, E)}$$

Hence, the total general matrix element  $M^{ij}$  is given by

$$M^{ij} = (k_i^2 - E) \delta_{ij} \frac{4\pi S_n^2}{\Omega} e^{i(\vec{k}_j - \vec{k}_i) \cdot \vec{r}_n} \left\{ \frac{g_{\ell}(|\vec{k}_j - \vec{k}_i| S_n)}{|\vec{k}_j - \vec{k}_i|} (\vec{k}_i \cdot \vec{k}_j - E) + \sum_{\ell=0}^{\infty} (2\ell+1) P_{\ell}(\vec{k}_i \cdot \vec{k}_j) g_{\ell}(k_i S_n) g_{\ell}(k_j S_n) \frac{R'_{n\ell}(S_n, E)}{R_{n\ell}(S_n, E)} \right\} \quad (2.6)$$

Having determined the general matrix element the problem now is to find the characteristic energies for which

$$\text{Det} (H - E)_{ij} = 0$$

Examination of the matrix element shows an explicit energy dependence through the terms  $(\vec{k}_i \cdot \vec{k}_j - E)$  and an intrinsic dependence through the radial function  $R_{n\ell}(\rho, E)$  and its derivative  $R'_{n\ell}(\rho, E)$ . Both types of dependence appear in the diagonal and off-diagonal terms. This type of problem cannot be solved exactly and the method which will be employed

here will be to choose an interesting energy range and examine the behavior of the determinant<sup>†</sup> as the energy is incremented in small steps through this range. To determine the variation of energy with wave vector it is necessary to repeat the calculation with enough different wave vectors so a meaningful plot of energy versus wave vector can be obtained.

## CHAPTER III

### THE NEUTRAL CALCULATION

The actual calculation of the energy bands for Cadmium Oxide was accomplished by modifying a set of computer programmes published by Loucks (1967). These programmes had been designed to perform relativistic or nonrelativistic calculations on a number of simple crystal structures. Their application required only a few basic input parameters physically describing the crystal. Unfortunately, they were limited for use on crystals containing only one type of atom. They also required atomic charge densities published by Liberman (1965) and these were not available to us at the time of this calculation. Because of these two limitations, a non-relativistic calculation for Cadmium Oxide required making many changes to the programmes. These can best be described by considering the complete set of programmes as consisting of three separate blocks, each making use of information obtained from the one before it. The first block calculates the crystal potential which is used by the second block to obtain the logarithmic derivatives and these are used in the third to evaluate the determinant.

#### The Potential

For a crystal consisting of neutral atoms the potential is created by superimposing atomic potentials  $V_A(r)$  and then adding a correction for the exchange energy. The atomic electronic potentials  $V_A(r)$  were obtained by numerically solving Poisson's equation (in atomic units)

$$\nabla^2 V_A(r) = -8\pi\sigma(r) \quad (3.1)$$

and this in turn requires atomic charge densities  $\sigma(r)$ . These charge densities were calculated from wave-functions tabulated by Herman and Skillman (1963). The wave-functions were determined for the occupied orbitals of ground state neutral atoms by a self-consistent Hartree-Fock calculation incorporating Slater's (1951) average free electron exchange approximation.

$$V_{ex}(r) = -6 \left( \frac{3}{8\pi} \sigma(r) \right)^{1/3} \quad (3.2)$$

The wave-functions are tabulated as a function of a common variable  $x$  for all elements. This variable corresponds to the value of the usual radial variable  $r$  (Bohr units) scaled by the cube root of the atomic number ( $Z$ ).

$$x = r/\mu$$

where

$$\begin{aligned} \mu &= \frac{1}{2} \left( \frac{3\pi}{4} \right)^{2/3} Z^{-1/3} \\ &= .88534138 Z^{-1/3} \end{aligned}$$

Since the atomic wave-functions are known to vary most rapidly for small  $r$  (and hence  $x$ ), and then decrease smoothly in value for large values of  $r$ , Herman and Skillman chose to calculate them at points on a linearly expanding mesh. This approach provides a suitable combination of both numerical accuracy and computer time efficiency. From an initial value of zero, the variable  $x$  is incremented by steps of .01 for the first ten intervals. The increment size is then doubled and continues to double after each successive ten interval block.

The functions  $P_{n\ell}(r)$  listed in the tables are related

to the atomic radial wave-function  $R_{nl}(r)$  as follows

$$P_{nl}(r) = r R_{nl}(r)$$

and the  $P_{nl}(r)$  are normalized to unity.

$$\text{ie.} \quad \int_0^{\infty} [P_{nl}(r)]^2 dr = 1$$

This is the same as the function tabulated by Liberman (mentioned earlier in this section) and will yield charge densities on the Herman Skillman (H.S) grid

$$\sigma_{HS}(r) = \sum_{\text{OCCUPIED ORBITALS}} B_{nl} (P_{nl}(r))^2$$

where  $B_{nl}$  is the number of electrons in the orbital defined by the quantum numbers  $n$  and  $l$ .

Since the logarithmic derivatives require numerical integration of the radial Schroedinger equation (2.3) the computer programmes for this calculation are based on an exponentially expanding scale

$$r = e^{x_0 + Jx\Delta}$$

Where  $x_0$  fixes the starting point some small distance from the origin;  $J$  takes on successive values 1,2,3, .....; and  $\Delta$  is an arbitrary step size which must satisfy the constraints set by the desired numerical accuracy and computer time available. For this calculation  $x_0 = -8.85$  and  $\Delta = .05$  were found to be satisfactory. This mesh has the effect of creating many more points near the origin ( $r < .01$ ) than the H.S grid and expanding the step size much more rapidly for large distances ( $r > 1.0$ ). Since the points on the two

meshes do not coincide, it was necessary to interpolate the densities from the linear to the exponential grid. In the region between the origin and the first non-zero H.S charge density, a parabolic interpolation was used. This is justified since for small  $r$  the radial wave-function  $R(r)$  is proportional to  $r^l$ . In this region the  $1s$  orbital is expected to dominate, yielding  $l=0$ . The required charge density follows from

$$\begin{aligned} [r R_{n0}(r)]^2 &\approx [r (a r^0)]^2 \\ &= a r^2 \end{aligned}$$

where "a" is the parameter to be fitted. For points beyond the first non-zero H.S charge density a linear interpolation was used.

The results of this interpolation were tested for oxygen against charge densities derived from analytic self-consistent field functions obtained by Clementi (1962) for neutral first row atoms using Slater type orbitals as basis functions. These charge densities were derived in the same fashion as those from the H.S wave-function. As can be seen from table (3.1) Clementi's Charge densities are not as large as those of Herman and Skillman for  $r \leq 2.0$ , but are larger for  $r > 2.0$ . The Clementi charge density does not, in fact, become zero for any value of  $r < 100.0$ . Considering the differences shown in table (3.1), the results of the comparison shown in table (3.2) may be judged to be fairly good. This comparison also reduced the possibility of overlooking programming errors in this part of the calculation.

These charge densities obtained in this fashion for oxygen

and cadmium were now used in the numerical solution of equation (3.1). The substitution

$$W = e^{x/a} V_A$$

reduces Poisson's equation to one containing only the second derivative

$$W'' = \frac{1}{4} W - 8\pi e^{\frac{x}{a}} \sigma(x)$$

Following Louck's (1967),  $W$  was expanded in Taylor series about an arbitrary point to obtain a set of finite difference equations and a recursion relation between neighbouring points was then introduced. The boundary condition requiring  $W$  to remain finite at the origin was used to determine the coefficients of the recursion relation. This recursion relation was then used in conjunction with the condition that  $V_A(r) = \frac{4\pi}{r}$  for large  $r$  to evaluate  $W$  at the last point on the grid and then at each successive point from the outer region inwards.

It is necessary to calculate the crystal potential as seen from the site of a cadmium atom and then from the site of an oxygen atom. This is done by superimposing the contributions from the surrounding shells of atoms using the method proposed by Lowden (1956). The number of atoms per shell and the distance of each shell from the central atom are listed for the case of a cadmium atom in table (3.3). The contribution from six shells was found to give a sufficiently converged result.

The exchange correction was now added using Slater's free exchange approximation given by

$$V_{ex}(r) = -6\alpha \left( \frac{3\sigma(r)}{8\pi} \right)^{1/3} \quad (3.3)$$

COMPARISON OF HERMAN SKILLMAN AND CLEMENTI  
CHARGE DENSITIES ON H.S. GRID (RHS)

\* \* \*

Table (3.1)

RHS	R	H.S.	Clementi
0.01	.004427	.073376	.071524
0.02	.008853	.273497	.266526
0.03	.013280	.573348	.558714
0.04	.017707	.949705	.925494
0.05	.022134	1.382246	1.347534
0.06	.026560	1.854731	1.808368
0.07	.030987	2.352034	2.294049
0.08	.035414	2.862423	2.792840
0.09	.039840	3.375990	3.294938
0.10	.044267	3.883666	3.792228
0.12	.053120	4.857491	4.747091
0.14	.061974	5.743687	5.618644
0.16	.070827	6.518471	6.383578
0.18	.079681	7.171661	7.030015
0.20	.088534	7.698820	7.554375
0.22	.097388	8.103112	7.958939
0.24	.106241	8.391174	8.249992
0.26	.115094	8.573686	8.436406
0.28	.123948	8.661028	8.528577
0.30	.132801	8.664824	8.537633
0.34	.150508	8.467962	8.351291
0.38	.168215	8.072724	7.963076
0.42	.185922	7.555906	7.447856
0.46	.203629	6.978609	6.866797
0.50	.221335	6.389239	6.267241
0.54	.239042	5.821131	5.683973
0.58	.256749	5.297343	5.141077
0.62	.274456	4.832286	4.653934
0.66	.292163	4.433516	4.231102
0.70	.309869	4.103897	3.875978
0.78	.345283	3.642863	3.364765
0.86	.380697	3.414853	3.091023
0.94	.416110	3.367801	3.007486
1.02	.451524	3.449832	3.063748
1.10	.486938	3.614918	3.213793
1.18	.522351	3.824816	3.419134
1.26	.557765	4.050589	3.649490
1.34	.593179	4.270482	3.882224
1.42	.628592	4.469457	4.101267
1.50	.664006	4.638688	4.295901
1.66	.734833	4.868533	4.589028
1.82	.805661	4.950202	4.742761
1.98	.876488	4.899626	4.766117
2.14	.947315	4.742741	4.680597
2.30	1.018143	4.509233	4.511346
2.46	1.088970	4.224072	4.282492

COMPARISON OF HERMAN SKILLMAN AND CLEMENTI  
CHARGE DENSITIES ON LOUCK'S GRID

\* \* \*

Table (3.2)

x	$R=e^x$	H.S.	Clementi
-8.80	.00015	.00008	.00008
-8.55	.00019	.00014	.00014
-8.25	.00026	.00025	.00026
-7.95	.00035	.00048	.00047
-7.65	.00047	.00088	.00085
-7.35	.00064	.00155	.00160
-7.05	.00086	.00281	.00290
-6.75	.00117	.00513	.00527
-6.45	.00158	.00935	.00954
-6.15	.00213	.01704	.01723
-5.85	.00287	.03106	.03103
-5.55	.00388	.05659	.05563
-5.25	.00524	.11048	.09919
-4.95	.00708	.19348	.17551
-4.65	.00956	.32147	.30736
-4.35	.01290	.54806	.53090
-4.05	.01742	.92552	.90007
-3.75	.02351	1.52999	1.48816
-3.45	.03174	2.43951	2.37890
-3.15	.04285	3.72139	3.63422
-2.85	.05784	5.33033	5.22427
-2.55	.07808	7.05369	6.92227
-2.25	.10539	8.36379	8.22697
-1.95	.14227	8.55951	8.46806
-1.65	.19204	7.35611	7.25151
-1.35	.25924	5.23191	5.06890
-1.05	.34993	3.61289	3.31614
-0.75	.47236	3.54699	3.14335
-0.45	.63762	4.51263	4.15357
-0.15	.86070	4.91089	4.77120
+0.15	1.16183	3.90036	4.00692
+0.45	1.56831	2.17614	2.37454
+0.75	2.11700	.85354	.96633
+1.05	2.85765	.24124	.25827
+1.35	3.85742	.04320	.04770

In this case  $\sigma(r)$  is the crystal charge found by superimposing atomic charge densities in the same fashion as given earlier in this section for the atomic potentials. The value of  $\alpha$  was equal to unity for Slater's (1951) original calculation and this is the value used by Herman and Skillman (1965) in their work (see equation 3.2). However, Kohn and Sham (1965) showed that  $\alpha$  should perhaps be closer to two thirds. Later, Schwarz (1972) fitted the Hartree-Fock energies to determine

$\alpha$  values for the first forty-one elements. The oxygen  $\alpha$  is given as .74447 and the value .701 for cadmium can be found by a short extrapolation. The changes resulting from use of these different  $\alpha$ 's are shown in table (3.4). Since  $\alpha=1.0$  yielded a direct gap which was closer to the experimental direct gap (.167 rydbergs) than  $\alpha = 2/3$ , and since the atomic wave-functions had been calculated originally with  $\alpha=1.0$ , we chose to perform the remainder of the calculations in this work with  $\alpha=1.0$ . The resulting crystal potentials for neutral cadmium and oxygen atoms are listed in tables (3.5) and (3.6) respectively.

The intersphere potential  $V_c$  and the sphere radii required in the muffin tin approximation are calculated by plotting these potentials in opposite directions from origins separated by half the cube edge ( $\frac{a}{2} = 4.4364 \text{ a.u.}$ ). The value of the potential at the point of intersection is taken as the intersphere potential. The distance from the origin of the cadmium potential to the intersection point determines the cadmium sphere radius and the oxygen sphere radius is (4.436 -  $S_{cd}$ ) a.u. This procedure is illustrated in Figure (3.1)

and the resulting values are:

$$V_c = -.975 \text{ ryd.}$$

$$S_{cd} = 2.435 \text{ a.u.}$$

$$S_{ox} = 2.000$$

These sphere radii must be converted into points on the exponential grid. Since the grid points are fixed and separated by a few tenths of an atomic unit at this distance, accurate determination of the sphere radii is only necessary for the intersphere potential.

Table (3.3)

TYPE OF ATOM IN SHELL	POSITION	NUMBER IN SHELL	DISTANCE
Cadmium	(0,0,0)	1	0.0
Oxygen	(1,0,0)	6	0.50000000
Cadmium	(1,1,0)	12	0.70710678
Oxygen	(1,1,1)	8	0.86602540
Cadmium	(2,0,0)	6	1.00000000
Oxygen	(2,1,0)	24	1.11803399
Cadmium	(2,1,1)	24	1.22474487
Cadmium	(2,2,0)	12	1.41421356

Number of atoms and distance from central cadmium atom of surrounding shells. The distance is measured in units of the lattice cube edge  $a = 8.8728$  a.u. .

Table (3.4)

Comparison of results obtained through the variation of the  $\alpha$  value in the exchange correction given by equation (3.3).

	<u>Kohn &amp; Sham</u>	<u>Shwarz</u>	<u>Slater</u>
$\alpha$ for oxygen	.666	.744	1.0
$\alpha$ for cadmium	.666	.701	1.0
Cd. radius (a.u.)	2.45	2.41	2.43
Ox. radius (a.u.)	1.98	2.02	2.00
$V_c$ (rydbergs)	-.66	-.72	-.975
Direct Gap (ryd)	.513		.264

Table (3.5)  
CADMIUM POTENTIAL FOR NEUTRAL CRYSTAL

$\rho$	$-V(\rho)$	$\rho$	$-V(\rho)$	$\rho$	$-V(\rho)$	$\rho$	$-V(\rho)$
.000151	636456.7	.000526	182040.6	.001836	51849.11	.006409	14543.36
.000158	605395.3	.000553	173141.4	.001936	49299.53	.006737	13812.69
.000166	575848.8	.000581	164676.2	.002026	46874.32	.007083	13117.71
.000175	547743.3	.000611	156623.8	.002133	44567.40	.007446	12456.60
.000184	521008.6	.000642	148964.2	.002242	42373.01	.007828	11827.70
.000193	495577.7	.000675	141678.1	.002357	40285.67	.008229	11229.56
.000203	471387.0	.000710	134747.4	.002478	38300.23	.008651	10660.67
.000213	448376.2	.000746	128154.7	.002605	36411.67	.009095	10119.63
.000224	426487.6	.000784	121883.6	.002739	34615.05	.009561	9605.103
.000236	405666.6	.000825	115918.2	.002879	32905.90	.010051	9115.325
.000248	385861.0	.000867	110243.9	.003027	31279.99	.010567	8649.312
.000261	367021.3	.000911	104846.2	.003182	29733.55	.011108	8206.188
.000274	349100.5	.000958	99711.89	.003345	28261.85	.011678	7784.845
.000288	332053.6	.001007	94827.92	.003517	26862.13	.012277	7384.233
.000303	315838.2	.001059	90182.14	.003697	25530.59	.012906	7003.365
.000319	300413.6	.001113	85762.95	.003887	24263.93	.013568	6641.267
.000335	285741.2	.001170	81559.28	.004086	23059.00	.014264	6297.033
.000352	271784.4	.001230	77560.64	.004296	21912.78	.014995	5969.636
.000370	258508.4	.001294	73757.02	.004516	20822.42	.015764	5658.278
.000389	245879.8	.001360	70138.91	.004748	19785.22	.016572	5362.338
.000409	233867.1	.001430	66697.27	.004991	18798.74	.017422	5080.950
.000430	222440.2	.001503	63423.49	.005247	17860.52	.018315	4813.376
.000452	211570.7	.001580	60309.38	.005516	16968.03	.019254	4559.103
.000476	201231.3	.001661	57347.15	.005799	16119.06	.020241	4317.316
.000500	191326.1	.001746	54529.41	.006096	15311.51	.021279	4087.525

Table (3.5)  
 CADMIUM POTENTIAL FOR NEUTRAL CRYSTAL  
 \* \* \*

$\rho$	$-V(\rho)$	$\rho$	$-V(\rho)$	$\rho$	$-V(\rho)$	$\rho$	$-V(\rho)$
.0223	3869.131	.0780	887.5781	.2725	142.4104	.9512	11.5498
.0235	3661.546	.0820	832.2839	.2865	130.8740	1.000	10.1845
.0247	3464.299	.0862	779.9211	.3011	120.1383	1.051	8.9570
.0259	3276.818	.0907	730.4443	.3166	110.1774	1.105	7.8624
.0273	3098.734	.0953	683.6564	.3328	100.9417	1.161	6.8891
.0287	2929.586	.1002	639.4565	.3499	92.3827	1.221	6.0252
.0301	2768.893	.1053	597.7036	.3678	84.4646	1.284	5.2634
.0317	2616.258	.1108	558.2956	.3867	77.1158	1.349	4.5920
.0333	2471.306	.1164	521.0954	.4065	70.3273	1.419	4.0013
.0350	2333.696	.1224	486.0240	.4274	64.0570	1.491	3.4831
.0368	2203.061	.1287	452.9530	.4493	58.2492	1.568	3.0332
.0387	2079.029	.1353	421.8052	.4723	52.8980	1.648	2.6391
.0407	1961.401	.1422	392.4772	.4965	47.9680	1.733	2.2942
.0428	1849.759	.1495	364.8925	.5220	43.4159	1.822	1.9951
.0450	1743.882	.1572	338.9722	.5488	39.2777	1.915	1.7405
.0473	1643.480	.1652	314.6313	.5769	35.4802	2.013	1.5177
.0497	1548.278	.1737	291.8098	.6065	32.0075	2.117	1.3342
.0523	1458.046	.1826	270.4267	.6376	28.8389	2.225	1.1796
.0550	1372.524	.1920	250.3683	.6703	25.9462	2.339	1.0529
.0578	1291.480	.2018	231.6355	.7046	23.2948	2.459	.9551
.0608	1214.704	.2122	214.0941	.7408	20.8653	2.585	.8858
.0639	1141.966	.2231	197.7156	.7788	18.6354	2.718	.8444
.0672	1073.077	.2345	182.4108	.8187	16.6053	2.857	.8326
.0706	1007.837	.2465	168.1354	.8607	14.7506		
.0742	946.0634	.2593	154.8124	.9048	13.0739		

Table (3.6)  
OXYGEN POTENTIAL FOR NEUTRAL CRYSTAL  
\* \* \*

$p$	$-V(p)$	$p$	$-V(p)$	$p$	$-V(p)$	$p$	$-V(p)$
.000151	106122.2	.000526	30386.01	.001836	8687.286	.006409	2470.928
.000158	100945.1	.000553	28902.81	.0001930	8262.341	.006737	2349.099
.000166	96020.72	.000581	27491.94	.002029	7858.121	.007083	2233.189
.000175	91336.47	.000611	26149.88	.002133	7473.615	.007446	2122.910
.000184	86880.68	.000642	24873.27	.002242	7107.862	.007828	2017.989
.000193	82642.20	.000675	23658.93	.002357	6759.947	.008229	1918.167
.000203	78610.43	.000710	22503.81	.002478	6429.000	.009651	1823.195
.000213	74775.29	.000746	21405.02	.002605	6114.193	.009095	1732.960
.000224	71127.19	.000784	20359.82	.002739	5814.740	.009561	1647.198
.000236	67657.02	.000825	19365.60	.002879	5529.892	.010051	1565.588
.000248	64356.09	.000867	18419.87	.003027	5258.936	.010567	1487.931
.000251	61216.14	.000911	1750.26	.003182	5001.195	.011108	1414.037
.000274	58229.33	.000958	16664.52	.003345	4756.24	.011678	1343.725
.000283	55388.19	.001007	15850.52	.003517	4522.810	.012277	1276.821
.000303	52685.62	.001059	15076.22	.003697	4300.971	.012906	1213.161
.000319	50114.85	.001113	14339.69	.003887	4089.951	.013568	1152.641
.000335	47669.45	.001170	13639.07	.004086	3889.223	.014264	1095.118
.000352	43343.33	.001230	12072.62	.004296	3698.285	.014995	1040.377
.000370	43130.64	.001294	12338.68	.004516	3516.750	.015764	988.2866
.000389	41025.88	.001360	11735.65	.004748	3344.160	.016572	938.7172
.000409	39023.76	.001430	11162.04	.004991	3179.940	.017422	891.5487
.000430	37119.29	.001503	10616.40	.005247	3023.686	.018315	846.7125
.00452	35307.69	.001580	10097.37	.005516	2875.015	.019254	804.0671
.000476	33584.46	.001661	9603.655	.005799	2733.561	.020241	763.4850
.000500	31945.26	.001746	9134.018	.006096	2598.976	.021279	724.8676

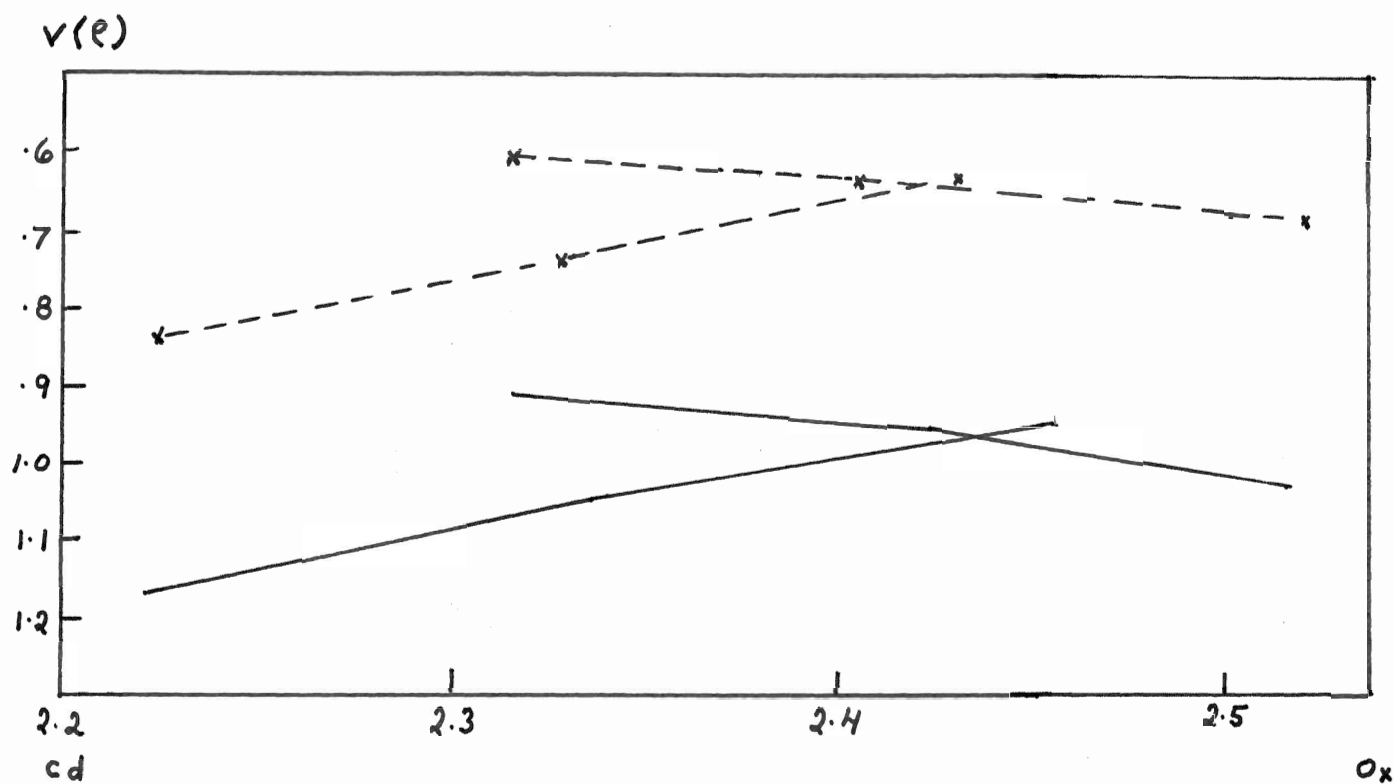
Table (3.6)  
OXYGEN POTENTIAL FOR NEUTRAL CRYSTAL  
\* \* \*

p	V(e)	p	V(e)	p	V(e)	p	V(e)
.0223	688.1298	.0780	1177.2230	.2725	36.0759	.9512	4.3460
.0235	653.0233	.0820	167.2895	.2865	33.5453	1.000	3.9167
.0247	619.9679	.0862	157.8570	.3011	31.1640	1.051	3.5247
.0259	588.3429	.0907	148.8998	.3166	28.9307	1.105	3.1679
.0273	558.2642	.0953	140.3959	.3328	26.8354	1.161	2.8438
.0287	529.6537	.1002	132.3226	.3499	24.8644	1.221	2.5504
.0301	502.4316	.1053	124.6654	.3678	23.0312	1.284	2.2860
.0317	476.5372	.1108	117.3937	.3867	21.3112	1.349	2.0487
.0333	451.9069	.1164	110.5024	.4065	19.7118	1.419	1.8377
.0350	428.4753	.1224	103.9646	.4274	18.2185	1.491	1.6490
.0368	406.1875	.1287	97.7649	.4493	16.8246	1.568	1.4842
.0387	384.9877	.1353	91.8877	.4723	15.5289	1.646	1.3383
.0407	364.8222	.1422	86.3153	.4965	14.3175	1.733	1.2161
.0428	345.6419	.1495	81.0501	.5220	13.1870	1.822	1.1116
.0450	327.3980	.1572	76.0502	.5488	12.1321	1.915	1.0280
.0473	310.6429	.1652	71.3235	.5769	11.1460	2.013	.9649
.0497	293.5438	.1737	66.8463	.6065	10.2250	2.117	.9211
.0523	277.8607	.1826	62.6104	.6376	9.3653	2.225	.8980
.0550	262.9367	.1920	58.6021	.6703	8.5627	2.339	.8977
.0578	248.7483	.2018	54.8113	.7046	7.8131	2.459	.9198
.0608	235.2691	.2122	51.2269	.7408	7.1203	2.585	.9670
.0639	222.4462	.2231	47.8388	.7788	6.4729	2.718	1.0423
.0672	210.2582	.2345	44.6385	.8187	5.8760	2.857	1.1518
.0706	198.6875	.2465	41.6172	.8607	5.3232		
.0742	187.6741	.2592	38.7646	.9048	4.8135		

Figure 3.1

Plot of crystal potential (ryd.) vs. distance  
from nuclei (a.u.) . Cd potentials have positive  
slopes. The cadmium oxygen separation is 4.4364 a.u.  
The dotted lines are calculated with  $\alpha' = 2/3$  , the  
solid lines are calculated with  $\alpha = 1$

Fig. 3.1



### The Logarithmic Derivatives

The ratio  $\frac{R'_{nl}(S_n, E)}{R_{nl}(S_n, E)}$  contained in the general matrix element given by equation (2.6) is called the logarithmic derivative (L.D.) of the wave-function  $R_{nl}$ . These L.D's must be evaluated on both the oxygen and cadmium sphere surfaces.

The substitution  $Y = \sqrt{r} R(r)$  reduces the radial Schroedinger Equation (2.3) to one involving only the second derivative and on the exponential mesh the resulting equation is

$$Y'' = (e^{2x} (V_R(r) - E) + (l + \frac{1}{2})^2) Y \quad (3.4)$$

This is solved numerically using Numerov's method. The derivative of the resulting function is then determined at each step by using the finite difference approximation

$$Y'_j = (Y_{j-2} - 8Y_{j-1} + 8Y_{j+1} - Y_{j+2}) / (12\Delta)$$

The subscripts denote the various grid points and  $\Delta = .05$  for this calculation. The approximation

$$Y(x) = Y(x_1) e^{(l+1)(x-x_1)}$$

is used to give starting values at the origin.

The energy dependence contained within the L.D's requires that they be completely re-evaluated each time the energy is changed. In order to avoid this very time consuming process, the radial function and its derivative are calculated at selected points over the energy range of interest and the results are fitted by a polynomial of arbitrary degree for each  $l$  value. In this calculation, an eighth degree polynomial gave suitable convergence. The L.D's at the sphere surfaces are then available for all energies in this range by evaluating the function

$$LD_{\ell}(E) = \sum_{i=0}^8 \frac{(QD)_i E^i}{(QC)_i E^i}$$

The coefficients (QC)<sub>i</sub> are determined by fitting the radial function and the coefficients (QD)<sub>i</sub> are determined by fitting the derivative of the radial function.

The variation with energy of the L.D.'s for some  $\ell$  values for neutral cadmium and oxygen are shown in figure (3.2) and figure (3.3) respectively. The functions for  $\ell = 0, 1, 2$  are quite sensitive to energy change, but for  $\ell \geq 3$  the sensitivity decreases rapidly. Singularities arise in these functions whenever a node in the radial function moves to the sphere surface. These singularities can result in spurious roots or loss of roots and consequently the energies at which they occur must be known. The singularities in the oxygen L.D.'s are at  $E \approx 1.6$  ryd for  $\ell = 0$  and at  $E \approx 2$  ryd for  $\ell = 1$ . A singularity in the cadmium L.D.'s arises at  $E \approx -.8$  for  $\ell = 2$ .

### The Determinant

The general matrix element is given by equation (2.6). For the specific case of cadmium oxide this becomes

$$\begin{aligned} M^{ij} = & (k_i^2 - E) \delta_{ij} \left[ \frac{4\pi S_{cd}^2}{\Omega} e^{i(\vec{k}_j - \vec{k}_i) \cdot \vec{r}_{cd}} \left\{ \frac{P_{\ell}(|\vec{k}_j - \vec{k}_i| S_{cd})}{(|\vec{k}_j - \vec{k}_i|)} (\vec{k}_i \cdot \vec{k}_j - E) \right. \right. \\ & + \left. \sum_{\ell=0}^{12} (2\ell+1) P_{\ell}(\hat{k}_i \cdot \hat{k}_j) f_{\ell}(k_i S_{cd}) f_{\ell}(k_j S_{cd}) LD_{\ell}(E, S_{cd}) \right\} \\ & + \frac{4\pi S_{ox}^2}{\Omega} e^{i(\vec{k}_j - \vec{k}_i) \cdot \vec{r}_{ox}} \left\{ \frac{P_{\ell}(|\vec{k}_j - \vec{k}_i| S_{ox})}{(|\vec{k}_j - \vec{k}_i|)} (\vec{k}_i \cdot \vec{k}_j - E) \right. \\ & + \left. \sum_{\ell=0}^{12} (2\ell+1) P_{\ell}(\hat{k}_i \cdot \hat{k}_j) f_{\ell}(k_i S_{ox}) f_{\ell}(k_j S_{ox}) LD_{\ell}(E, S_{ox}) \right] \end{aligned}$$

FIGURE 3.2

L.D'S for Neutral Cd

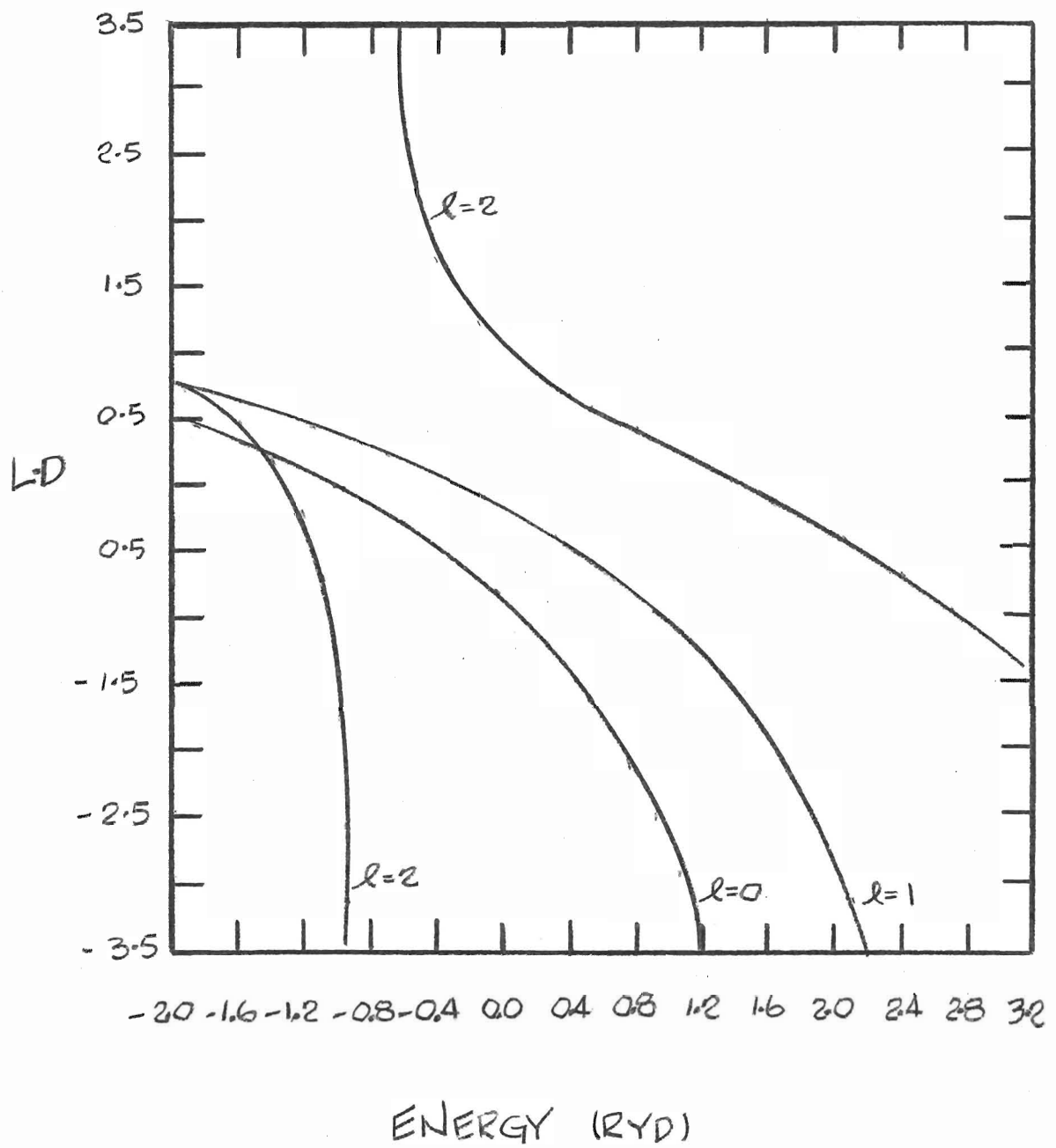


FIGURE 3.2

L.D.'S for Neutral Cd

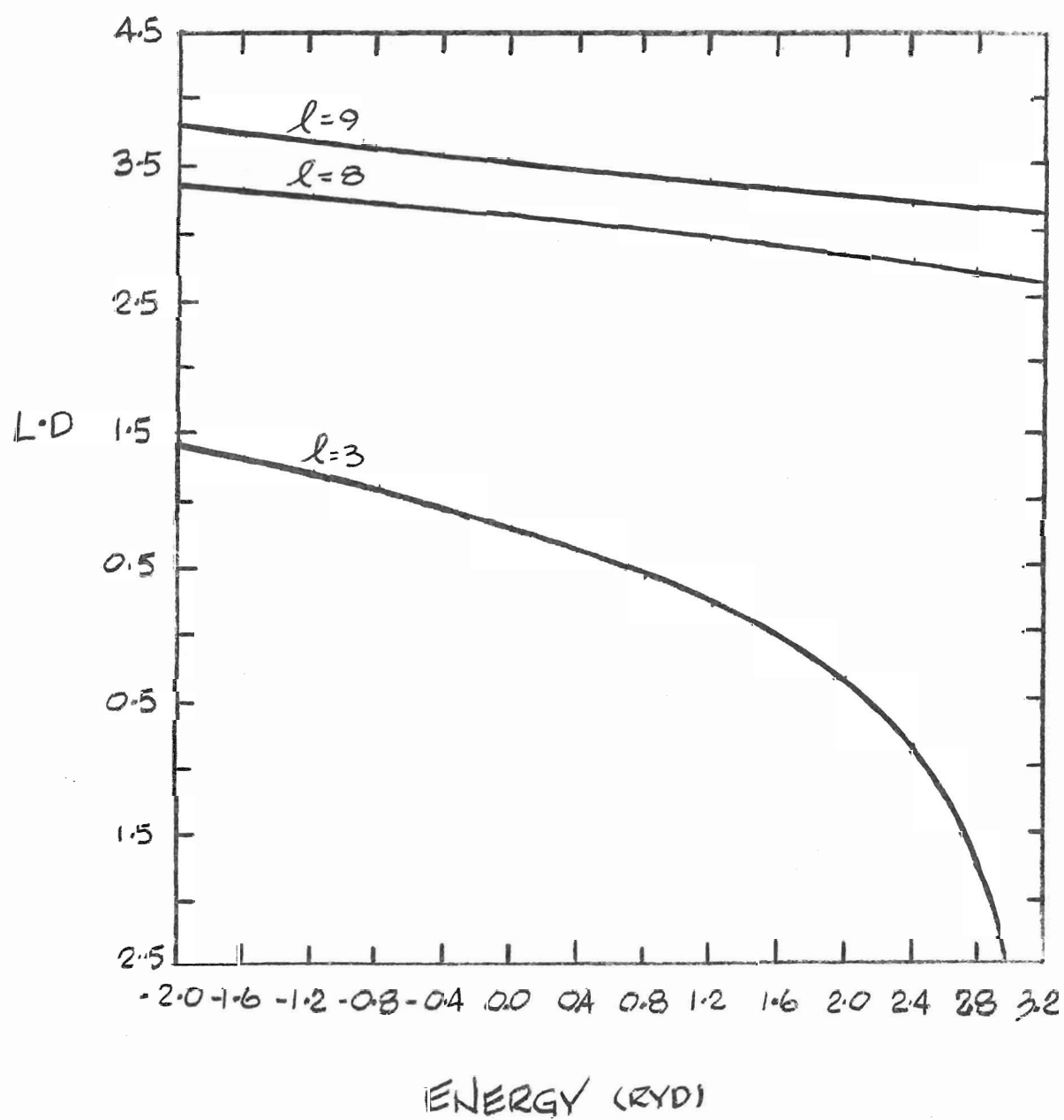


FIGURE 3.3

L.D.'S for Neutral Oxygen

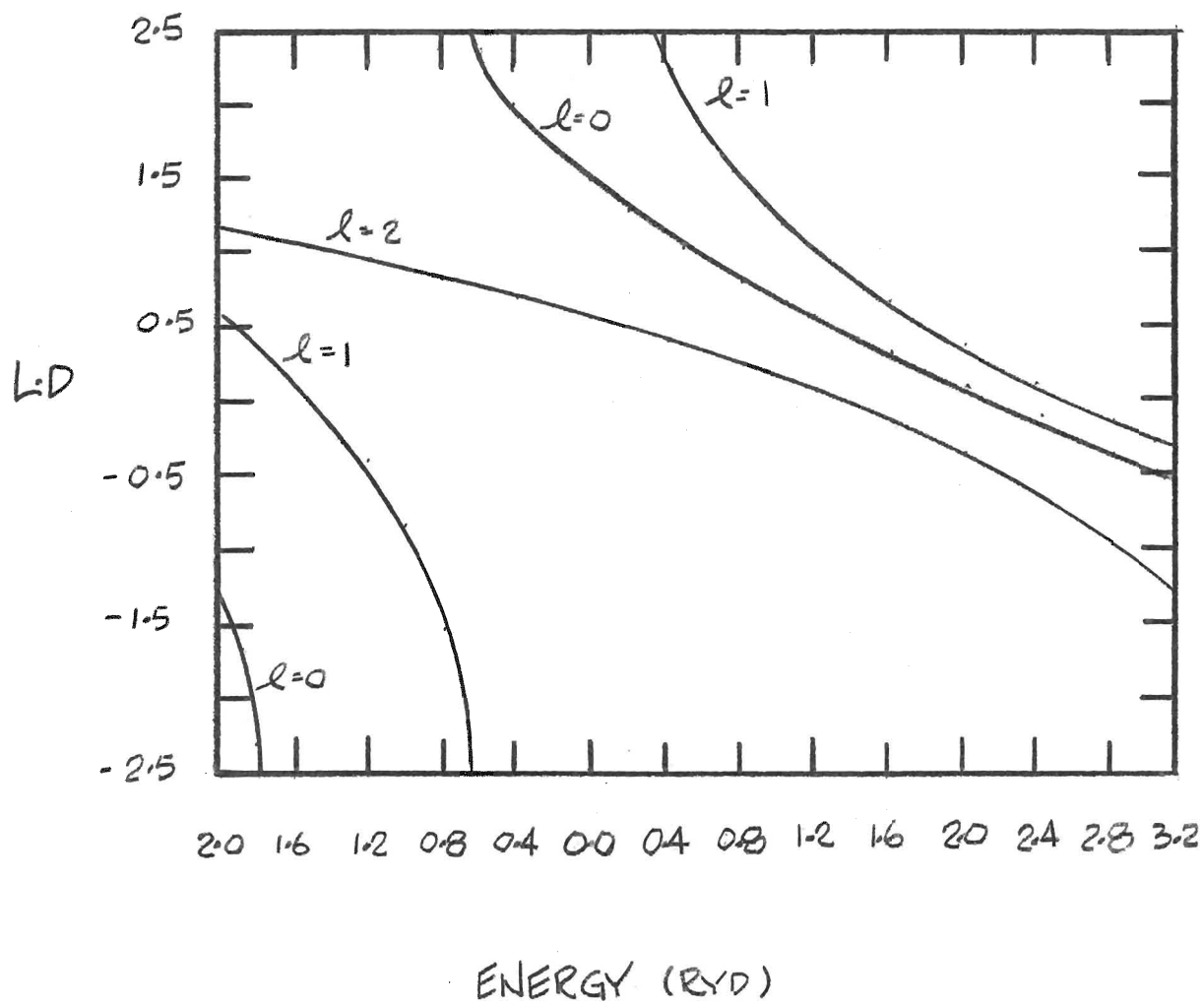
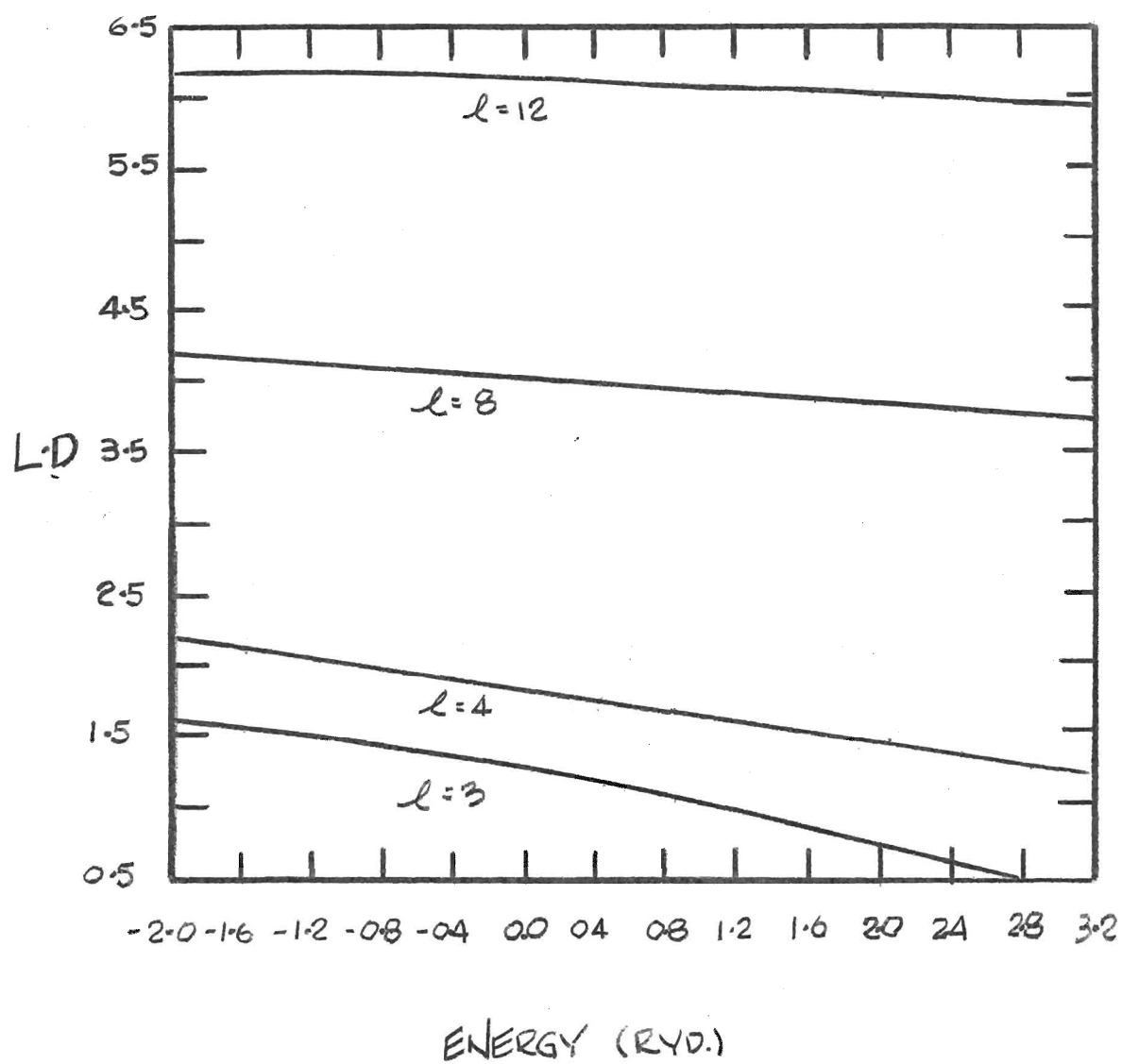


FIGURE 3.3

L.D.'S for Neutral Oxygen



This differs from equation (2.6) in that the infinite sum over  $l$  values has in practice been restricted to a finite number. In this calculation  $l = 12$  gave sufficient convergence. The spherical Bessel functions  $j_l$  and the Legendre polynomials  $P_l$  were calculated from recursion relations. The imaginary factors  $e^{i(\vec{k}_j - \vec{k}_i) \cdot \vec{r}_{ox}}$  and  $e^{i(\vec{k}_j - \vec{k}_i) \cdot \vec{r}_{cd}}$  can both be made real by choosing the origin on either an oxygen or a cadmium atom site. This ensures that these factors are always +1 or -1.

The eigenvalues are determined by evaluating the determinant for an interesting range of energy and picking out those energies which correspond to zeroes. Energy steps of .01 will generally locate these zeroes but as mentioned in the discussion on the L.D's, particular care must be taken when investigating energies close to those creating singularities.

The number of APW's required to give converged eigenvalues depends on the wave vector in question. Generally 65 basis functions give accuracy within a few thousandths of a rydberg; although for points of low symmetry 113 basis functions will cause a decrease of about three one thousandths of a rydberg from that obtained with 65. The eigenvalues at  $\Gamma$  and convergence with increasing number of APW's is shown in table (3.7). The direct gap (  $\Gamma_1 - \Gamma_{15}$  ) calculated with 65 APW's is -.2950 rydbergs.

TABLE 3.7

Illustration of convergence of energy (ryd.) eigenvalues  
at  $\Gamma$  by increasing number of APW's from 9 to 65.

TABLE 3.7  
NEUTRAL CALCULATION OF EIGENVALUES AT  $\Gamma$

	9	15	27	51	59	65
$\Gamma_1$	-1.0164	-1.0392	-1.0457	-1.0503	-1.0508	-1.0510
$\Gamma_{25}$	-0.0095	-0.0099	-0.0369	-0.0500	-0.0600	-0.0600
$\Gamma_{12}$		-0.001	-0.022	-0.040	-0.040	-0.0425
$\Gamma_{15}$	.2769	.1873	.1430	.1200	.1114	.1106
$\Gamma_1$	.4414	.4106	.4071	.4058	.4056	.4056

## THE IONIC CALCULATION

In order to fit the experimental direct gap of  $-0.1676 \pm 0.0037$  rydbergs, we chose to vary the ionicity of the cadmium and oxygen atoms. This was done by decreasing the number of electrons in the 5S shell of the cadmium atom and increasing the number by the same amount in the oxygen 2P shell but without changing the one electron orbitals. The amount of extra charge transferred to the oxygen atom (called the "ionicity" of the calculation) was varied continuously until a direct gap of  $0.1676$  rydbergs was obtained using an ionicity of  $0.277$ . The gap width was very sensitive to the degree of ionicity and for an ionicity of  $1.0$  the  $\Gamma_1$  and  $\Gamma_{15}$  points reversed positions to give a gap of  $0.0902$  rydbergs.

The cadmium charge density is probably not affected very much inside the 5S shell, but the effects on oxygen are relatively severe, ie. the 2P orbitals should be allowed to relax. This was apparent from a comparison of charge densities with those obtained from a calculation for ionic oxygen by Clementi (1965). Consequently this ionicity should be regarded as a parameterization only and not an indication of the crystal ionicity.

The introduction of ionicity into the calculation makes it necessary to adjust the crystal potential with a correction for the Madelung energy. This was done by accounting for the short range contributions through the superposition calculation mentioned in Chapter III, and then allowing for the effects of the ions outside the six-shells by including the appropriate fraction of the Madelung constant for Na Cl structures. The

resulting potentials are shown in tables (4.1) and (4.2) for cadmium and oxygen respectively.

These potentials were then used to calculate the sphere radii and intersphere potential using the method outlined previously in Chapter III in the section on the potential. The resulting values were

$$S_{cd} = 2.46 \text{ a.u.}$$

$$S_{ox} = 1.98 \text{ a.u.}$$

$$V_c = -.90 \text{ ryd.}$$

These values coupled with the potentials were used to calculate the logarithmic derivatives given in tables (4.3) and (4.4) for cadmium and oxygen respectively. The singularities occur at  $E = -.8245 \text{ ryd}$  ( $l = 0$ ) and  $E = -.0043 \text{ ryd}$  ( $l = 1$ ) for oxygen and  $E = -.1799 \text{ ryd}$  ( $l = 2$ ) for cadmium.

The energy eigenvalues at  $\Gamma$  were calculated and their variation with increasing number of basis functions was determined. Each of these eigenvalues may be related to a corresponding atomic orbital through the tight binding approximation. This relationship and the variation of eigenvalues with increasing number of basis functions is shown in table (4.5). The energy bands were then calculated in the  $\Sigma$ ,  $\Lambda$ , and  $\Delta$  directions from  $\Gamma$  to the zone boundary. Since it was found that the individual band shapes varied only slightly with increasing number of basis functions these bands were calculated using 65 instead of the more accurate 113 basis functions. This was necessary in order to keep the computer time and core requirements at a reasonable level. Having determined the

overall band shapes in the directions of interest and thus, having located the maxima and minima in the valence and conduction bands respectively, the gaps could be more accurately calculated using 113 basis functions. The bands determined from calculations using 65 basis functions are shown in figures (4.1), (4.2), and (4.3). Comparison of these results with those obtained by Maschke and Rössler (1968) shows the general features to be very similar. Both calculations suggest the possibility of the existence of  $\Gamma - L$  and  $\Gamma - \Sigma$  indirect gaps and in both the  $\Gamma - L$  gap is the smaller gap. The results of this work indicate the  $\Gamma - L$  gap is 1.32 eV and the  $\Gamma - \Sigma$  gap is 1.38 eV. These gaps have been calculated using 113 basis functions and consequently are more accurate and slightly larger than those shown in figures (4.1) and (4.2). The band ordering and general shape is also similar to Tewari's (1972) ionic calculation and Breeze and Perkin's LCAO calculation but there is a difference in the spacing of the  $\Gamma - L$  and  $\Gamma - \Sigma$  indirect gaps. In both of these works the  $\Gamma - \Sigma$  gap is smaller than the  $\Gamma - L$  gap. In all cases the gaps calculated in previous works are a few tenths of an eV smaller than the ones calculated here. Smaller gaps could result from any one of several areas. Different methods of constructing the crystal potential, the use of too few basis functions, or different methods of extracting the energy which gives a zero value to the determinant could all lead to differences of this magnitude.

The results of this calculation are quite different than those obtained by Tewari (1972) for neutral cadmium oxide which

suggest metallic behaviour and which have the position of the p and d bands reversed relative to each other. Only radical differences in the construction of the crystal potential would lead to a rearrangement of band position such as this. Because Tewari's calculation assumes a completely neutral crystal (ie. no ionic bonding), and because we have tried to incorporate ionicity into our calculation by fitting the direct optical gap it is not surprising to find such large differences in the band structures. In fact because the approximation of rigid orbitals causes the oxygen 2P energy to rise too quickly with increasing ionicity, our fitted ionicity value of .277 is probably more consistent with an ionic charge of 1 and this is why our results resemble her ionic calculation more than her neutral calculation.

All the previous workers have limited their band calculations to the  $\Sigma$ ,  $\Lambda$ , and  $\Delta$  symmetry directions and as was mentioned the results suggest the existence of two indirect gaps; one from the maximum in the  $\Sigma$  direction in the valence band to the minimum at  $\Gamma$  in the conduction band and the other from the maximum at  $L$  in the valence band to the minimum at  $\Gamma$  in the conduction band.

In order to be sure that both are local maxima in the valence band it is necessary to investigate the band behaviour around the points. This information is necessary since what appears to be a maximum in one direction may be only a saddle point in another. The density of states for a maximum and a saddle point is not the same as the density of states for two

Maxima and it is the density of states which determines the results seen experimentally. The density of states for two maxima and the density of states for a maximum and a saddle point are shown in figures (4.4a) and (4.4b).

In order to investigate the region around the maximum in the  $\Sigma$  direction it was necessary to first determine the wave-vector corresponding to this maximum value. This was done by incrementing the  $k_x$  and  $k_y$  components of the wave-vector by steps of .002 ( $\frac{2\pi}{a}$ ) to find a maximum energy and then using the two closest points to find a maximum value from a quadratic fit. This led to a value of  $\vec{k} = (.4588, .4588, 0)$  which yields the maximum energy of .3226 rydbergs in a calculation using 65 basis functions. The variation in energy in two directions perpendicular to each other and to the  $\Sigma$  axis was calculated and the results are shown in Table (4.6). Part (ii) of the table shows a decrease in energy for points in the  $k_x, k_y$  plane in a direction perpendicular to the  $\Sigma$  direction. This still suggests that  $(.4588, .4588, 0) \times (\frac{2\pi}{a})$  corresponds to a local maximum. However, moving in the  $\vec{k}_z$  direction from the maximum point it is apparent from the results shown in part (i) of Table (4.6A) that the energy eigenvalues are increasing. This tendency continues in this direction to a maximum of .3275 rydbergs at  $\vec{k} = (.4588, .4588, .50) \frac{2\pi}{a}$ . From this maximum, by moving towards the L point at the zone boundary it is possible to keep the energy rising continually until the maximum of .3290 rydbergs is obtained at L. Consequently the maximum in the  $\Sigma$  symmetry

axis is not a local maximum but is a saddle point with one increasing and two decreasing branches. Table (4.6B) gives the eigenvalues in two directions perpendicular to each other and to the  $\Lambda$  direction at  $L$ . The results indicate that

$L$  is an absolute maximum as was suggested by the previous workers.

In order to predict the optical properties of cadmium oxide it is necessary to know the shape of the valence and conduction bands around  $\Gamma$  and also the effective masses characterizing these bands and the maximum at  $L$  are required. The shapes and effective masses were determined from eigenvalues calculated for small changes in wave-vector around the points. The eigenvalues and effective masses in the three symmetry directions around  $\Gamma$  are listed for the conduction band in table (4.7) and for the valence band in table (4.8). The effective masses were calculated using a Taylor series expansion to approximate the band shape. Because of symmetry considerations only the even terms in the expansion were retained for all calculations but the longitudinal effective mass at  $L$ . These values coupled with the band shapes shown in figures (4.1), (4.2), and (4.3) show that the conduction band is parabolic and isotropic with the point at  $\Gamma$  being an absolute minimum. The valence band at  $\Gamma$  is anisotropic since the eigenvalues increase slowly in the  $\Lambda$  and  $\Sigma$  directions and decrease very slowly in the  $\Delta$  direction. The effective masses at  $L$  were calculated in the  $\Lambda$  direction which is the longitudinal

direction and in two transverse directions. Energies in the transverse directions were calculated for wave-vectors  $(.5+\Delta, .5-\Delta, .5)\frac{2\pi}{a}$  and  $(.5-\Delta, .5-\Delta, .5+2\Delta)\frac{2\pi}{a}$  where variation of  $\Delta$  generates different points in these two directions. The eigenvalues for various choices of  $\Delta$  and the resulting effective masses are shown in table (4.9).

Table (4.)  
 CADMIUM POTENTIAL FOR CRYSTAL WITH IONICITY = .277  
 \* \* \*

$\rho$	$-V(\rho)$	$\rho$	$-V(\rho)$	$\rho$	$-V(\rho)$	$\rho$	$-V(\rho)$
.000151	636456.7	.000526	182040.6	.001336	51849.12	.006409	14543.47
.000158	605395.3	.000553	173141.4	.001930	49299.55	.006737	13812.71
.000166	575848.8	.000581	164676.2	.002029	46874.34	.007083	13117.73
.000175	547743.3	.000611	156623.8	.002133	44567.42	.007446	12456.62
.000184	521008.6	.000642	148964.2	.002242	42373.03	.007828	11927.72
.000193	495577.7	.000675	141678.2	.002357	40285.68	.008229	11229.57
.000203	471387.1	.000710	134747.4	.002478	38300.25	.009651	10660.69
.000213	448376.2	.000746	128154.7	.002605	36411.69	.009095	10119.65
.000224	426487.7	.000784	121883.6	.002738	34615.07	.009561	9605.122
.000236	405666.6	.000825	115918.3	.002879	32905.92	.010051	9115.345
.000248	385861.0	.000867	110243.9	.003027	31280.01	.010567	8649.331
.000261	367021.3	.000911	104846.3	.003182	29733.27	.011108	8206.207
.000274	349100.5	.000958	99711.91	.003345	28261.87	.011678	7784.864
.000288	332053.7	.001007	94827.94	.003517	26862.15	.012277	7384.251
.000303	315838.2	.001059	90182.16	.003697	25530.61	.012906	7003.384
.000319	300413.6	.001113	85762.97	.003887	24263.95	.013568	6641.286
.000335	285741.2	.001170	81559.30	.004086	23059.01	.014264	6297.052
.00035	271784.5	.001230	77560.66	.004296	21912.80	.014995	5969.655
.000370	258508.4	.001294	73757.04	.004516	20822.44	.015764	5658.297
.000389	245879.8	.001360	70138.93	.004748	19785.24	.016572	5362.356
.000409	233867.1	.001430	66697.29	.004991	18798.76	.017422	5080.969
.000430	222440.2	.001503	63423.51	.005247	17860.53	.018315	4813.394
.000452	211570.7	.001580	60309.40	.005516	16968.05	.019254	4549.122
.000476	201231.3	.001661	573447.17	.005799	16119.08	.020241	4317.334
.000500	191396.1	.001746	54529.43	.006096	15311.53	.021279	4087.543

Table (4.1)  
 CADMIUM POTENTIAL FOR CRYSTAL WITH IONICITY = .277

$\rho$	$-V(\rho)$	$\rho$	$-V(\rho)$	$\rho$	$-V(\rho)$	$\rho$	$-V(\rho)$
.0223	3869.150	.0780	887.5942	.2725	142.4216	.9512	11.5475
.0235	3661.565	.0820	832.2998	.2865	130.8849	1.000	10.1814
.0247	3464.317	.0862	779.9369	.3011	120.1489	1.051	8.9530
.0259	3276.836	.0907	730.4600	.3166	110.1877	1.105	7.8575
.0273	3098.752	.0953	683.6720	.3328	100.9516	1.161	6.8832
.0287	2929.604	.1002	639.4719	.3499	92.3923	1.221	6.0181
.0301	2768.911	.1053	597.7189	.3678	84.4639	1.284	5.2550
.0317	2616.275	.1108	558.3107	.3867	77.1248	1.349	4.5820
.0333	2471.323	.1167	521.1104	.4065	70.3359	1.419	3.9894
.0350	2333.714	.1224	486.0388	.4274	64.0652	1.491	3.4689
.0368	2203.079	.1287	452.9677	.4493	58.2570	1.568	3.0165
.0387	2079.046	.1353	421.8197	.4723	52.9054	1.648	2.6193
.0407	1961.419	.1422	392.4916	.4965	47.9748	1.733	2.2709
.0428	1849.776	.1495	364.9067	.5220	43.4220	1.822	1.9678
.0450	1743.899	.1572	338.9862	.5488	39.2831	1.915	1.7089
.0473	1643.897	.1652	314.6452	.5769	35.4849	2.013	1.4814
.0497	1548.295	.1737	291.8234	.6065	32.0115	2.117	1.2934
.0523	1458.064	.1826	270.4401	.6376	28.8421	2.225	1.1341
.0550	1372.541	.1920	250.3815	.6703	25.9589	2.339	1.0030
.0578	1291.497	.2018	231.6484	.7046	23.2967	2.459	.9011
.0608	1214.720	.2122	214.1067	.7408	20.8666	2.585	.8284
.0639	1141.982	.2231	197.7279	.7788	18.6360	2.718	.7841
.0672	1073.094	.2345	182.4229	.8187	16.6052	2.857	.7699
.0706	1007.854	.2465	168.1472	.8607	14.7498		
.0742	946.0796	.2592	154.8239	.9048	13.0724		

Table (7.2)  
 OXYGEN POTENTIAL FOR CRYSTAL WITH IONICITY = .277  
 \* \* \*

$P$	$-V(P)$	$P$	$-V(P)$	$P$	$-V(P)$	$P$	$-V(P)$
.000151	106121.5	.000526	30385.57	.001836	8686.847	.006409	2470.489
.000158	100944.7	.000553	28902.37	.001930	8261.902	.006737	2348.660
.000166	96020.28	.000581	27491.50	.002029	7857.682	.007083	2232.750
.000175	91336.04	.000611	26149.44	.002133	7473.176	.007446	2122.471
.000184	86880.24	.000642	24872.83	.002242	7107.423	.007828	2017.550
.000193	82641.76	.000675	23658.49	.002357	6759.508	.008229	1917.728
.000203	78609.99	.000710	22503.37	.002478	6428.561	.009651	1822.756
.000213	74774.85	.000746	21404.58	.002605	6113.754	.009095	1732.521
.000224	71126.76	.000784	20359.38	.002739	5814.301	.009561	1646.759
.000236	67656.58	.000825	19365.16	.002879	5529.453	.010051	1565.149
.000248	64355.65	.000867	18419.43	.003027	5259.497	.010567	1487.493
.000261	61215.70	.000911	17519.82	.003182	5000.756	.011108	1413.599
.000274	58228.89	.000958	16664.08	.003345	4755.585	.011678	1343.286
.000288	55387.75	.001007	15850.08	.003517	4522.371	.012277	1276.382
.000303	52685.18	.001059	15075.78	.003697	4300.532	.012906	1212.722
.000319	50114.41	.001113	14339.25	.003887	4089.512	.013568	1152.202
.000335	47669.02	.001170	13638.63	.004086	3888.784	.014264	1094.679
.000352	45342.89	.001230	12972.18	.004296	3697.846	.014995	1039.939
.000370	43130.21	.001294	12338.24	.004516	3516.311	.015764	987.8477
.000389	41025.44	.001360	11735.21	.004748	3343.722	.016572	938.2784
.000409	39023.32	.001430	11161.60	.004991	3179.501	.017422	891.1099
.000430	37118.85	.001503	10615.96	.005247	3023.247	.018315	846.2737
.000452	35307.26	.001580	10096.63	.005516	2874.576	.019254	803.6283
.000476	33584.02	.001661	9603.21	.005799	2731.122	.020241	763.0463
.000500	31944.82	.001746	9133.580	.006096	2598.538	.021279	724.4288

Table (4.2)  
 OXYGEN POTENTIAL FOR CRYSTAL WITH IONICITY = .277  
 \* \* \*

$P$	$-V(P)$	$P$	$-V(P)$	$P$	$-V(P)$	$P$	$-V(P)$
.0223	687.6910	.0780	176.7852	.2725	35.6681	.9512	4.1084
.0235	652.7646	.0820	166.8519	.2865	33.1418	1.000	3.6895
.0247	619.5292	.0862	157.4195	.3011	30.7651	1.051	3.13086
.0259	587.9041	.0907	148.4626	.3166	28.5369	1.105	2.9631
.0273	557.8255	.0953	139.9589	.3328	26.4070	1.161	2.6505
.0287	529.2150	.1002	131.8858	.3499	24.4817	1.221	2.3686
.0301	501.9929	.1053	124.2289	.3678	22.6542	1.284	2.1156
.0317	476.0985	.1108	116.9576	.3867	20.9401	1.349	1.8895
.0333	451.4682	.1164	110.0667	.4065	19.3466	1.419	1.6897
.0350	428.0366	.1224	103.5293	.4274	17.8590	1.491	1.5117
.0368	405.7488	.1287	97.3301	.4493	16.4709	1.568	1.3572
.0387	384.5491	.1353	91.4535	.4723	15.1807	1.648	1.2212
.0407	364.3835	.1422	85.8818	.4965	13.9750	1.733	1.1082
.0428	345.2034	.1495	80.6173	.5220	12.8503	1.822	1.0122
.0450	326.9595	.1572	75.6184	.5488	11.8012	1.915	.9365
.0473	309.6044	.1652	70.8926	.5769	10.8214	2.013	.8806
.0497	293.1054	.1737	66.4166	.6065	9.9070	2.117	.8433
.0523	277.4223	.1826	62.1820	.6376	9.0543	2.225	.8263
.0550	262.4983	.1920	58.1753	.6703	8.2592	2.339	.8318
.0578	248.3100	.2018	54.3863	.7046	7.5176	2.459	.8598
.0608	234.8309	.2122	50.8040	.7408	6.8332	2.585	.9129
.0639	222.0081	.2231	47.4182	.7788	6.1946	2.718	.9943
.0672	209.8201	.2345	44.2205	.8187	5.6072	2.857	1.1097
.0706	198.2495	.2465	41.2022	.8607	5.0642		
.0742	187.2362	.2592	38.3530	.9048	4.5648		

TABLE (4.3)

Logarithmic Derivatives for Cadmium  $l = 0, 1, 2, 3$   
for ionicity = .277

E	$l = 0$	$l = 1$	$l = 2$	$l = 3$
-3.5	1.1627	1.3842	1.4450	1.7787
-3.3	1.0976	1.3184	1.3849	1.7335
-3.1	1.0301	1.2527	1.3215	1.6873
-2.9	.9600	1.1866	1.2541	1.6401
-2.7	.8869	1.1195	1.1819	1.5918
-2.5	.8104	1.0509	1.1032	1.5424
-2.3	.7302	.9806	1.0160	1.4919
-2.1	.6458	.9081	.9167	1.4400
-1.9	.5567	.8332	.7992	1.3867
-1.7	.4621	.7554	.6519	1.3320
-1.5	.3613	.6743	.4495	1.2756
-1.3	.2532	.5896	.1243	1.2174
-1.1	.1367	.5006	-.5876	1.1573
-0.9	.0101	.4060	-4.7465	1.0951
-0.7	-.1284	.3078	4.2454	1.0305
-0.5	-.2816	.2023	2.0707	.9633
-0.3	-.4527	.0897	1.4999	.8931
-0.1	-.6462	-.0314	1.2023	.8197
0.1	-.8683	-.1624	.9988	.7425
0.3	-1.1280	-.3053	.8372	.6610
0.5	-1.4381	-.4623	.6967	.5745
0.7	-1.8186	-.6366	.5672	.4822
0.9	-2.3017	-.8321	.4430	.3829
1.1	-2.9429	-1.0543	.3207	.2751
1.3	-3.8469	-1.3107	.1975	.1570
1.5	-5.2388	-1.6122	.0717	.0257

TABLE (4.3)

Logarithmic Derivatives for Cadmium  $\rho = 4, 8, 12$   
for ionicity = .277

E	$\rho = 4$	$\rho = 8$	$\rho = 12$
-3.5	2.1116	3.5555	5.0690
-3.3	2.0732	3.5315	5.0522
-3.1	2.0342	3.5074	5.0353
-2.9	1.9947	3.4832	5.0183
-2.7	1.9545	3.4588	5.0013
-2.5	1.9138	3.4342	4.9842
-2.3	1.8724	3.4095	4.9671
-2.1	1.8303	3.3847	4.9499
-1.9	1.7875	3.3597	4.9326
-1.7	1.7440	3.3345	4.9153
-1.5	1.6998	3.3092	4.8979
-1.3	1.6547	3.2837	4.8805
-1.1	1.6088	3.2581	4.8630
-0.9	1.5620	3.2323	4.8454
-0.7	1.5143	3.2063	4.8277
-0.5	1.4656	3.1802	4.8100
-0.3	1.4159	3.1539	4.7922
-0.1	1.3650	3.1274	4.7744
0.1	1.3130	3.1007	4.7565
0.3	1.2598	3.0739	4.7385
0.5	1.2052	3.0468	4.7204
0.7	1.1493	3.0196	4.7023
0.9	1.0918	2.9922	4.6841
1.1	1.0328	2.9646	4.6659
1.3	.9720	2.9368	4.6475
1.5	.9094	2.9088	4.6291

TABLE (4.4)

Logarithmic Derivatives for Oxygen  $\beta = 0, 1, 2, 3$   
for ionicity = .277

E	$\beta = 0$	$\beta = 1$	$\beta = 2$	$\beta = 3$
-3.5	.7862	1.1595	1.5966	2.0279
-3.3	.6801	1.0927	1.5509	1.9907
-3.1	.5605	1.0221	1.5043	1.9530
-2.9	.4230	.9473	1.4567	1.9148
-2.7	.2610	.8673	1.4081	1.8761
-2.5	.0638	.7811	1.3585	1.8368
-2.3	-.1870	.6872	1.3078	1.7971
-2.1	-.5254	.5836	1.2559	1.7567
-1.9	-1.0226	.4675	1.2027	1.7158
-1.7	-1.8570	.3349	1.1482	1.6743
-1.5	-3.6381	.1793	1.0923	1.6321
-1.3	-10.7018	-.0092	1.0348	1.5893
-1.1	22.7867	-.2485	.9757	1.5458
-0.9	6.4193	-.5717	.9148	1.5016
-0.7	3.9575	-1.0500	.8521	1.4567
-0.5	2.9311	-1.8697	.7873	1.4110
-0.3	2.3481	-3.7209	.7203	1.3645
-0.1	1.9588	-13.0595	.6509	1.3171
0.1	1.6707	13.1859	.5788	1.2689
0.3	1.4417	4.8450	.5039	1.2198
0.5	1.2499	3.0669	.4258	1.1696
0.7	1.0824	2.2587	.3443	1.1185
0.9	.9317	1.7754	.2588	1.0663
1.1	.7924	1.4391	.1691	1.0129
1.3	.6611	1.1810	.0746	.9584
1.5	.5352	.9685	-.0251	.9026

TABLE (4.4)

Logarithmic Derivatives for Oxygen  $l = 4, 8, 12$   
for ionicity = .277

E	$l = 4$	$l = 8$	$l = 12$
-3.5	2.4816	4.4134	6.4003
-3.3	2.4501	4.3942	6.3870
-3.1	2.4183	4.3750	6.3736
-2.9	2.3863	4.3557	6.3603
-2.7	2.3539	4.3363	6.3468
-2.5	2.3213	4.3169	6.3334
-2.3	2.2883	4.2974	6.3199
-2.1	2.2550	4.2778	6.3064
-1.9	2.2214	4.2581	6.2929
-1.7	2.1874	4.2384	6.2793
-1.5	2.1531	4.2186	6.2657
-1.3	2.1184	4.1987	6.2521
-1.1	2.0834	4.1787	6.2384
-0.9	2.0479	4.1587	6.2247
-0.7	2.0121	4.1386	6.2110
-0.5	1.9759	4.1184	6.1973
-0.3	1.9393	4.0981	6.1835
-0.1	1.9022	4.0777	6.1697
0.1	1.8648	4.0573	6.1558
0.3	1.8268	4.0368	6.1419
0.5	1.7884	4.0162	6.1280
0.7	1.7495	3.9955	6.1141
0.9	1.7101	3.9747	6.1001
1.1	1.6703	3.9539	6.0861
1.3	1.6298	3.9329	6.0721
1.5	1.5889	3.9119	6.0580

TABLE 4.5

Illustration of convergence of energy (ryd.) eigenvalues  
at  $\Gamma$  by increasing number of APW's from 9 to 113.

TABLE 4.5  
 IONICITY = .277

	9	27	65	89	113
$\Gamma_1$	-.8903	-.9185	-.9228	-.9230	-.9230
$\Gamma_{25'}$	-.0702	-.0999	-.1244	-.1249	-.1250
$\Gamma_{12}$			-.106	-.107	-.109
$\Gamma_{15}$	.4184	.2800	.2530	.2509	.2502
$\Gamma_1$	.4582	.4226	.4209	.4208	.4208

Expected Ordering From  
 Tight Binding Approximation

$O(2s) \rightarrow \Gamma_1$   
 $Cd(4d) \rightarrow \Gamma_{25'} + \Gamma_{12}$   
 $O(2p) \rightarrow \Gamma_{15}$   
 $Cd(5s) \rightarrow \Gamma_1$

Fig 4.1  
 $\Sigma$  DIRECTION

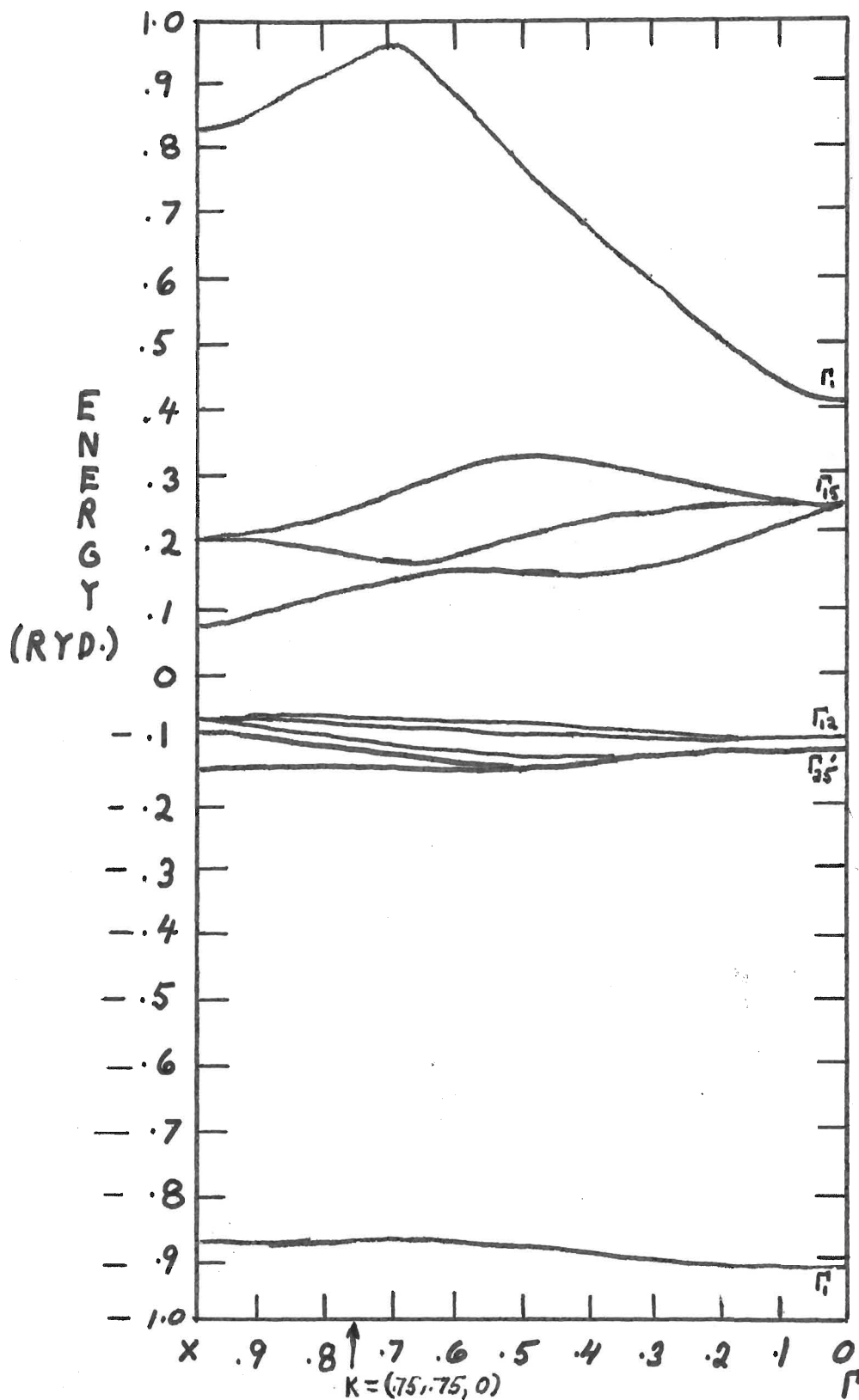
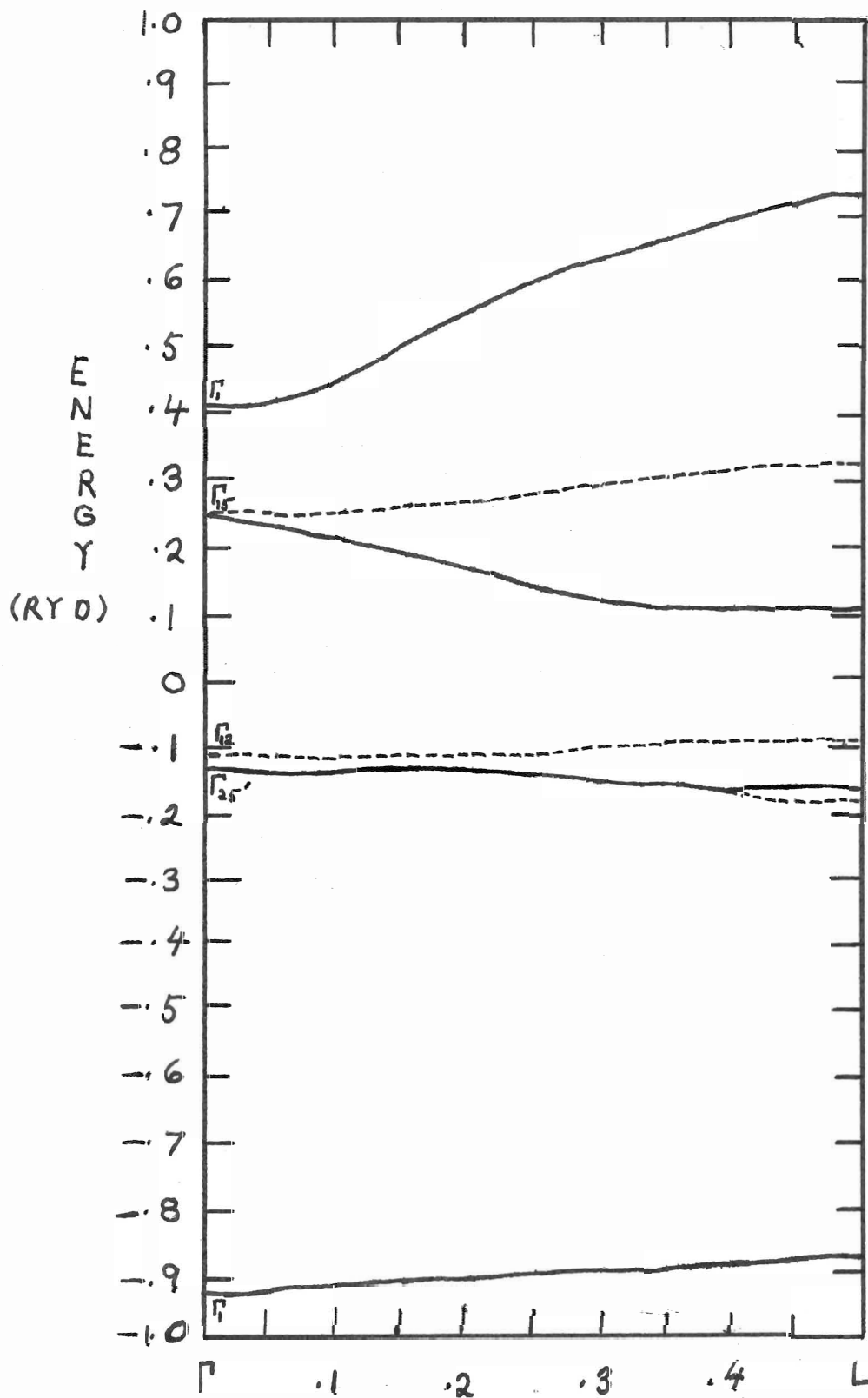


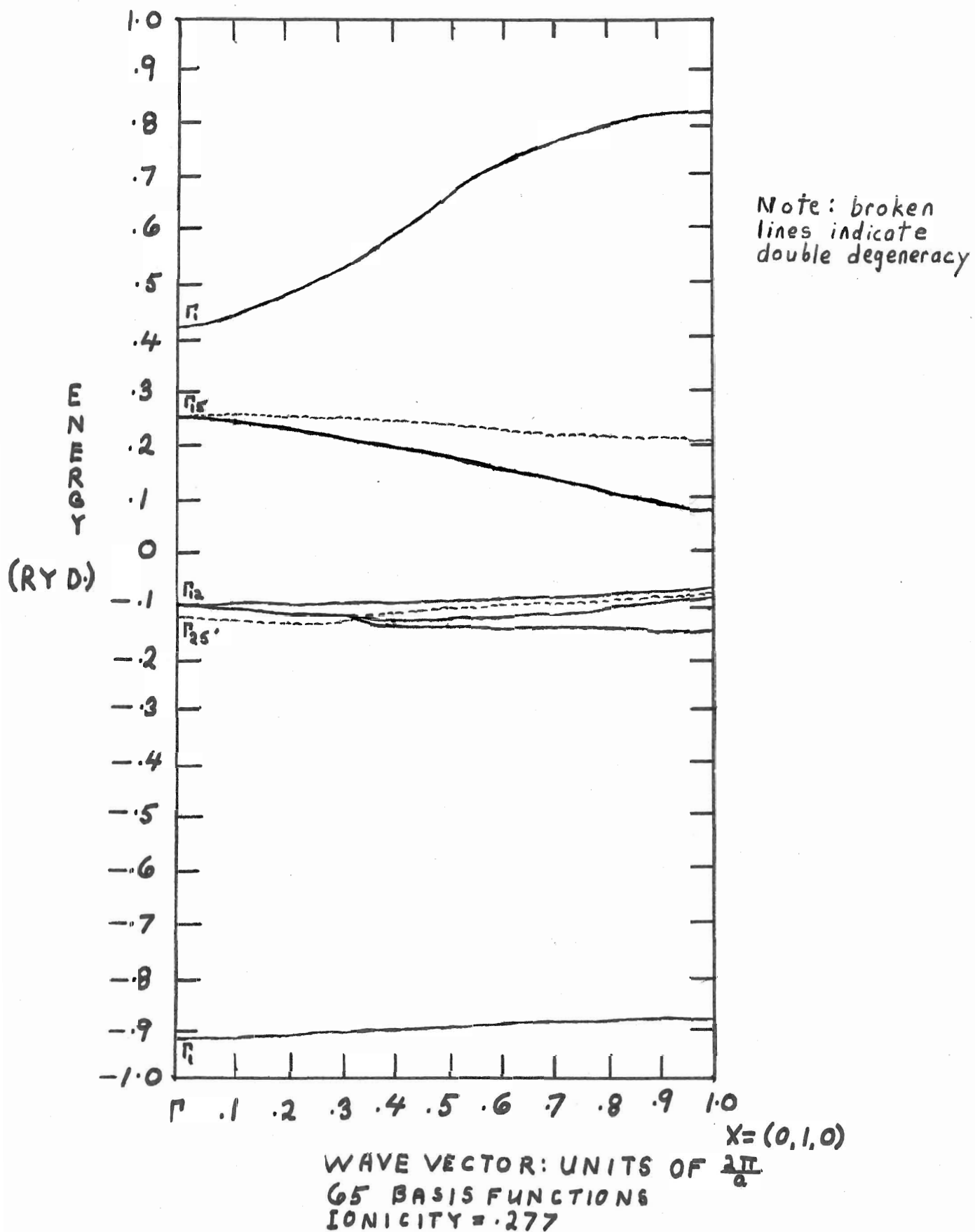
Fig 4.2  
 $\wedge$  Direction



NOTE: broken  
 lines indicate  
 double degeneracy.

WAVE VECTOR: UNITS OF  $\frac{2\pi}{a}$   
 65 BASIS FUNCTIONS  
 IONICITY = .277

Fig. 4.3  
 $\Delta$  DIRECTION



Figures 4.4a and 4.4b show a schematic plot of density of states  $D(\epsilon)$  in the valence band as a function of energy  $\epsilon$ .  $\epsilon_L$  is the energy at  $L$  and  $\epsilon_{\Sigma}$  is the energy of the maximum in the  $\Sigma$  symmetry axis.

Figure 4.4a corresponds to the case of two local maxima, one at  $L$  and a smaller one in the  $\Sigma$  axis.

Figure 4.4b corresponds to the case of one maximum at  $L$  and a saddle point in the  $\Sigma$  axis.

Fig. 4.4 a

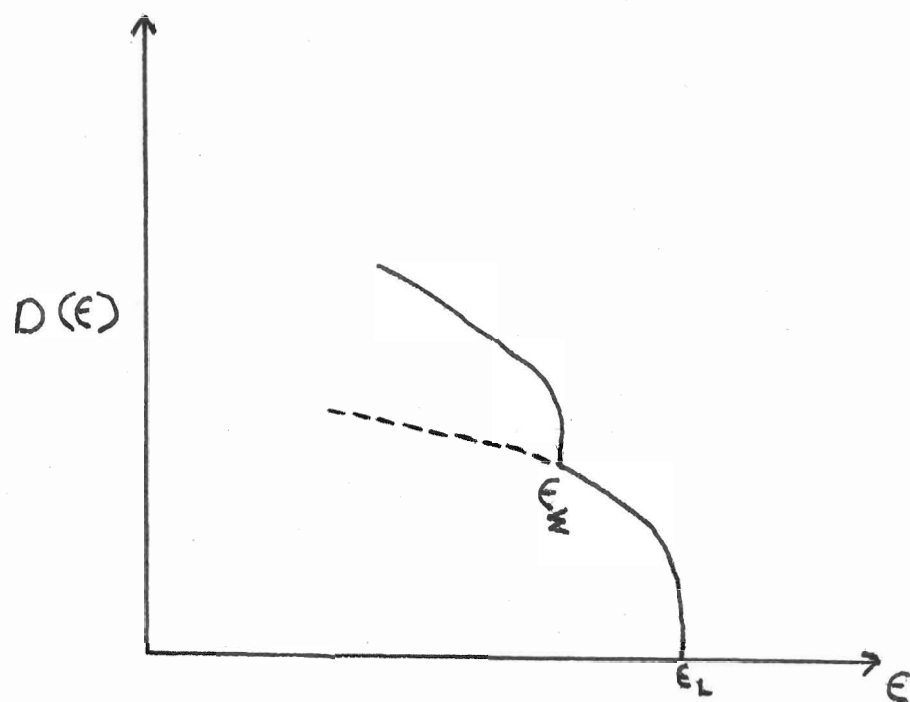


Fig. 4.4 b

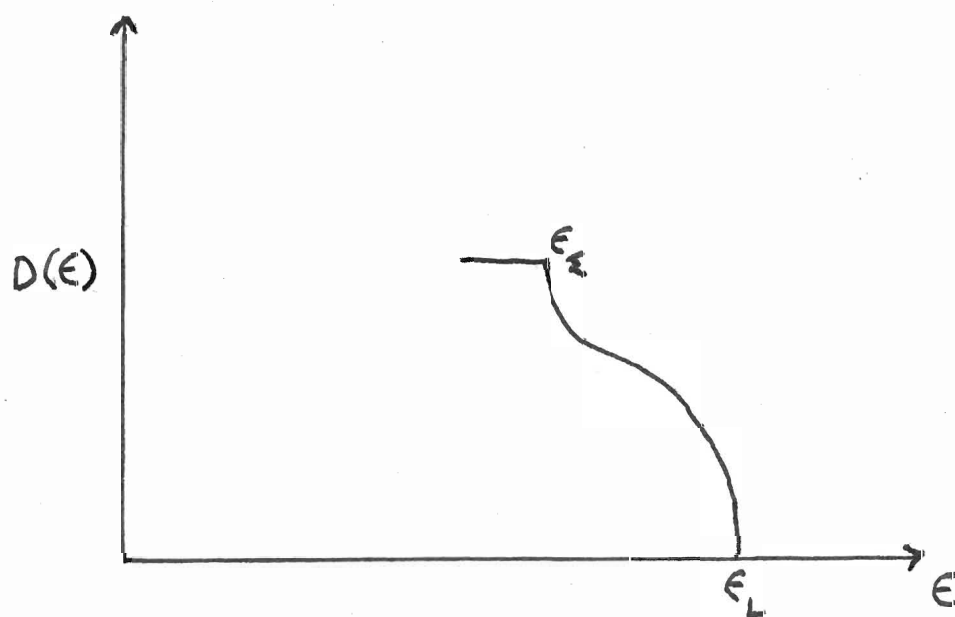


TABLE 4.6

A) Eigenvalues perpendicular to the maximum in the  $\hat{z}$  directioni) Stepping in  $\hat{z}$  direction perpendicular to  $\hat{z}$ 

Wave - Vector	Energy Rydbergs
(.4588 , .4588 , 0 )	.3226
(.4588 , .4588 , .05 )	.3227
(.4588 , .4588 , .075 )	.3229
(.4588 , .4588 , .1 )	.3231
(.4588 , .4588 , .2 )	.3244
(.4588 , .4588 , .3 )	.3259
(.4588 , .4588 , .4 )	.3269
(.4588 , .4588 , .47 )	.3272
(.4588 , .4588 , .50 )	.3275
(.4588 , .4588 , .53 )	.3271
(.4588 , .4588 , .58 )	.3268
(.4588 , .4588 , .5824)	.3267

Stepping from local maximum (above) towards  $\hat{L}$ 

(.4588 , .4588 , .50 )	.3275
(.46 , .46 , .50 )	.3275
(.47 , .47 , .50 )	.3278
(.48 , .48 , .50 )	.3286
(.49 , .49 , .50 )	.3289
(.50 , .50 , .50 )	.3290

ii) Second direction from the  $\hat{z}$  maximum

Wave - Vector	Energy Rydbergs
(.4588 , .4588 , 0 )	.3226
(.5088 , .4088 , 0 )	.3183
(.5338 , .3838 , 0 )	.3132

B) Eigenvalues perpendicular to  $\hat{A}$  direction around  $\hat{L}$ 

i)	Wave - Vector	Energy Rydbergs
	(.5 , .5 , .5 )	.329
	(.55 , .45 , .5 )	.327
	(.6 , .4 , .5 )	.323
ii)	(.5 , .5 , .5 )	.329
	(.45 , .45 , .6 )	.325
	(.425 , .425 , .65)	.321

TABLE 4.7  
 Band Shapes and Effective Masses  
 of Conduction Band Around  $\Gamma$

Direction	Wave-Vector( $\frac{2\pi}{a}$ )	Energy (ryd)	Effective Mass
$\triangle$	(0, 0, 0)	.4208	.12
	(0, .05, 0)	.4257	
	(0, .1, 0)	.4389	
	(0, .2, 0)	.4836	
$\wedge$	( 0, 0, 0 )	.4208	.12
	(.05, .05, .05)	.4346	
	(.1, .1, .1)	.4679	
	(.15, .15, .15)	.5101	
$\approx$	( 0, 0, 0 )	.4208	.12
	(.05, .05, 0)	.4303	
	(.1, .1, 0)	.4546	
	(.15, .15, 0)	.4875	
	(.2, .2, 0)	.5250	

TABLE 4.8  
Band Shapes and Effective Masses  
of Valence Band Around  $\Gamma$

Direction Wave-Vector( $\frac{2\pi}{a}$ ) Energy (ryd) Effective Mass

$\Delta$	(0, 0, 0)	.2530	-3.46
	(0, .05, 0)	.2528	
	(0, .1, 0)	.2527	
	(0, .15, 0)	.2522	
	(0, .2, 0)	.2514	

$\Lambda$	(0, 0, 0)	.2530	.87
	(.05, .05, .05)	.2551	
	(.1, .1, .1)	.2608	
	(.15, .15, .15)	.2694	
	(.2, .2, .2)	.2800	

$\Sigma$	(0, 0, 0)	.2530	.85
	(.05, .05, 0)	.2546	
	(.1, .1, 0)	.2610	
	(.15, .15, 0)	.2701	
	(.2, .2, 0)	.2811	

EFFECTIVE MASSES AT  $L$ Longitudinal Direction

Wave-vector ( $\frac{\pi}{a}$ )	Energy (ryd)	Effective Mass
(.5, .5, .5)	.329157	-1.34
(.475, .475, .475)	.328318	
(.450, .450, .450)	.326742	
(.425, .425, .425)	.324364	
(.400, .400, .400)	.321246	

Transverse Directionsi)  $(.5+\Delta, .5-\Delta, .5)\frac{\pi}{a}$ 

$\Delta$	Energy	Effective Mass
0	.329157	-0.83
.05	.327693	
.10	.323919	

ii)  $(.5-\Delta, .5-\Delta, .5+2\Delta)\frac{\pi}{a}$ 

$\Delta$	Energy	Effective Mass
0	.329157	-1.01
.05	.325652	
.075	.321215	
.10	.317884	

## CHAPTER V

### DISCUSSION AND CONCLUSION

The aim of this work was to improve the calculation by varying the ionicity to fit the known experimental gap, to make a detailed study of the band shapes around the regions of interest, and to obtain effective masses characterizing these regions.

The value of .277 for the ionicity which was found to give eigenvalues at  $\Gamma$  which would fit the experimental direct gap is a considerable understatement as was mentioned in chapter IV. This aspect of the calculation could be greatly improved by self-consistently calculating the atomic wave-functions and the charge densities so the orbitals could change with the redistributed charge densities. The use of Slater's  $\chi\alpha$  exchange approximation in both the atomic and crystal potentials would also be an improvement which could be incorporated into this part of the calculation. It is felt however that the ionicity is a more realistic parameter to vary when fitting the direct gap than the intersphere potential which was used in previous work and hence the calculation is improved through this approach.

The conduction band at  $\Gamma$  was found to be parabolic and isotropic but the valence band at  $\Gamma$  is anisotropic, that is its curvature is different in the three symmetry directions and it may be described as having a fluted shape. The effective masses for these bands and those at L were calculated and the value  $m^* = .12 m_e$  for the conduction band at  $\Gamma$  agrees favourably with  $m^* = .14 m_e$  quoted by Koffyberg (1975).

The maximum in the  $\Sigma$  symmetry axis was found to be a saddle point and consequently there is only one absolute maximum in the valence band and this occurs at  $L = (.5, .5, .5) \frac{2\pi}{a}$ . The difference in energy between this maximum and the minimum in the conduction band at  $\Gamma$  is 1.32eV. While this is about .2eV higher than the indirect gaps that are found experimentally, the presence of only one maximum in the valence band should explain why the experimentalists are having such a difficult time locating two indirect gaps.

Apart from the improvement suggested for fitting the ionicity, the calculation still does not include either effects of correlation or the free carrier concentrations which exist in the real crystals and these could have a significant effect on the band structure. However, it is hoped that the new knowledge of the band shapes and effective masses plus the information that there is only one maximum in the valence band will aid in any future research on cadmium oxide.

## BIBLIOGRAPHY

1. Altwein, M., Finkenrath, H., Konak C., Stuke, J., and Zimmerer, G. (1968). Phys, Status Solidi 29, 203.
2. Breeze, A. and Perkins, P.G. (1973). Solid State Commun. 13, 1031.
3. Clementi, E. and C.C.J. Roothaan, and M. Yoshimine (1962). Phys. Rev 127, 1618.
4. Clementi, E. (1965). IBM Journal of Research and Development, Supplement 9, 2.
5. DeCicco, P.D. (1965). PhD Thesis., M.I.T. Dept of Physics (unpublished).
6. Herman, F., and Skillman, S. (1963). "Atomic Structure Calculations" Prentice-Hall, Englewood Cliffs, New Jersey.
7. Kocka, J. and Konak, C. (1971). Phys. Status Solidi 43, 731.
8. Koffyberg, F.P. (1975). Phys. Rev 13, 4470.
9. Köhler, H. (1972). Solid State Commun. 11, 1687.
10. Kohn, W. and Sham, L.J. (1965). Phys Rev. 140 A1133.
11. Liberman, D., Waber, J.T., and Cromer, D.T. (1965). Phys Rev. 137 A27.
12. Loucks, Terry (1967). "Augmented Plane Wave Method", Benjamin, New York.
13. Lowden, P.O. (1956). "Quantum Theory of Cohesive Properties of Solids" Adv. Phys., 5,1.
14. Maschke, K. and Rössler, U. (1968). Phys. Status Solidi 28, 577.
15. Powell, J.L. and Craseman, B. (1961). "Quantum Mechanics", Addison-Wesley, Reading, Mass.
16. Schwarz, K. (1972). Phys Rev B5, 2466.
17. Slater, J.C. (1937). Phys Rev 51, 846.
18. Slater, J.C. (1951). Phys Rev 81, 385.
19. Slater, J.C. (1974). "The Self-Consistent Field for Molecules and Solids". Vol. 4, McGraw-Hill, New York.
20. Tewari, S. (1973). Solid State Commun. 12, 437.